Physics of Fast Processes in Scintillators

Andrey Vasil'ev

Skobeltsyn Institute of Nuclear Physics, Lomonosov Moscow State University,
Moscow, Russia

e-mail: anv@sinp.msu.ru

НИИЯФ МГУ

FAST

Intelum

CRYSTAL CLEAR

Why do we need fast timing and how fast should it be?

Event pile-up at high luminosity

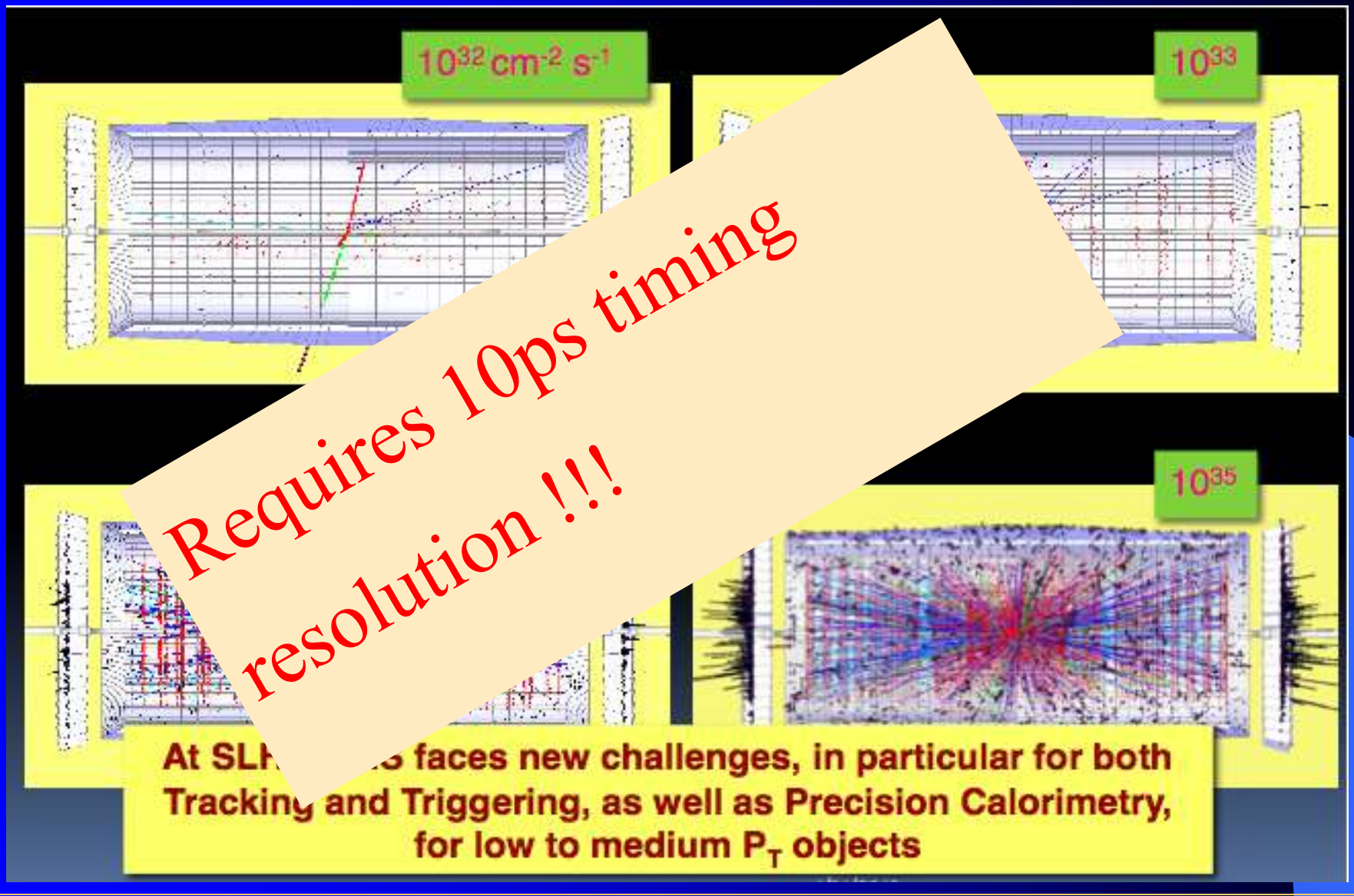

EndoTOFPET-US: Why TOF?

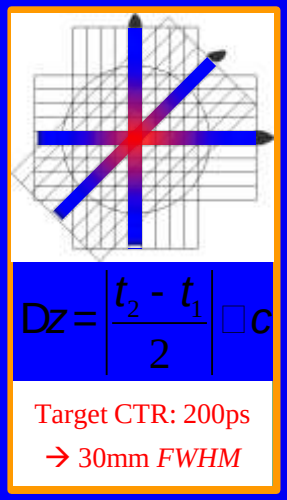

$$Dz = \left| \frac{t_2 - t_1}{2} \right| \cdot c$$

Target CTR: 200ps
→ 30mm *FWHM*

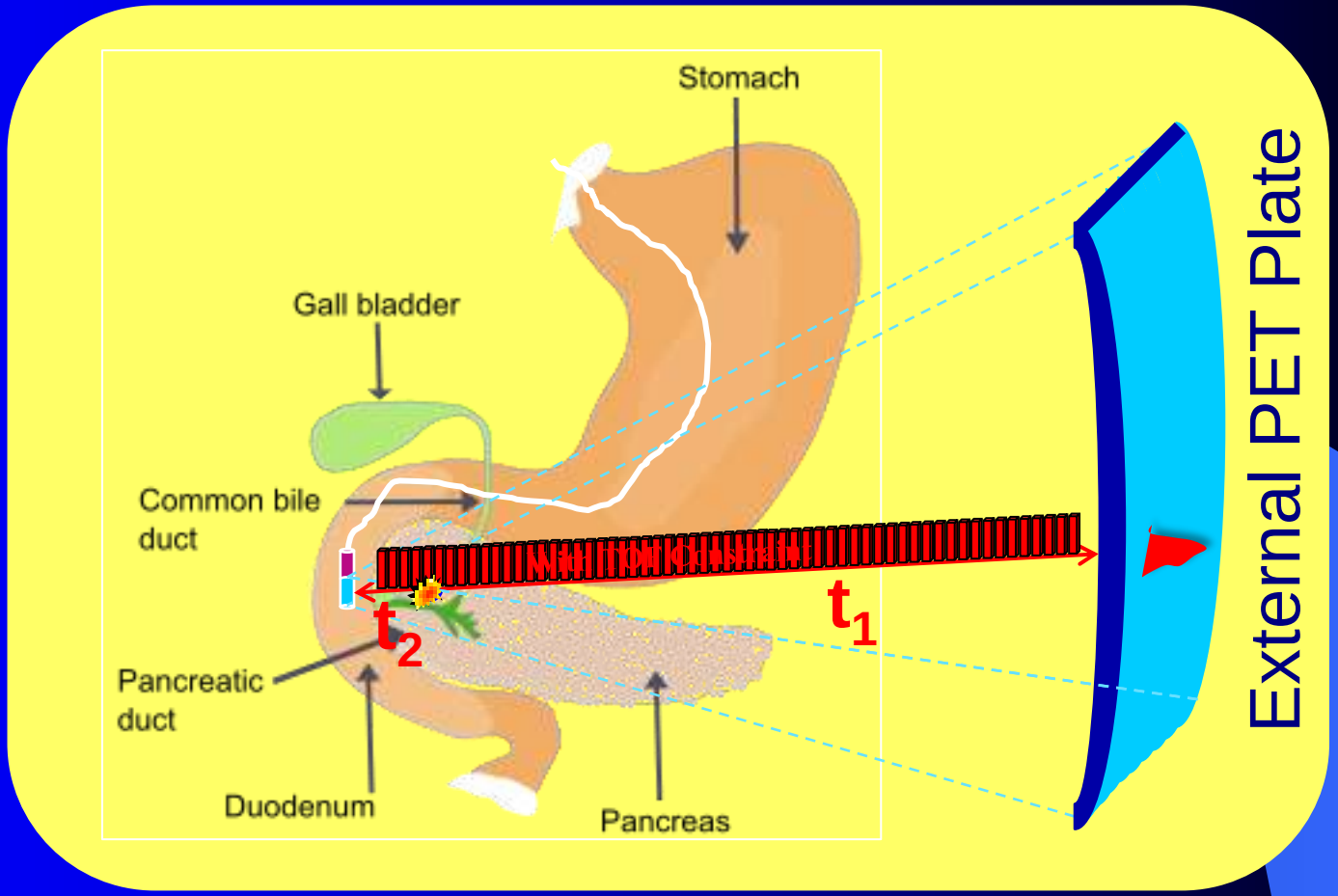

Why fast timing in PET scanners?

- TOF for rejecting background events (event collimation)
  - Requires 200ps TOF resolution
- TOF for improving image S/N
  - 100ps TOF resolution improves S/N by a factor of ≈ 5
- TOF for direct 3D information
  - Requires 1 to 2mm resolution along LOR → 10ps TOF resolution

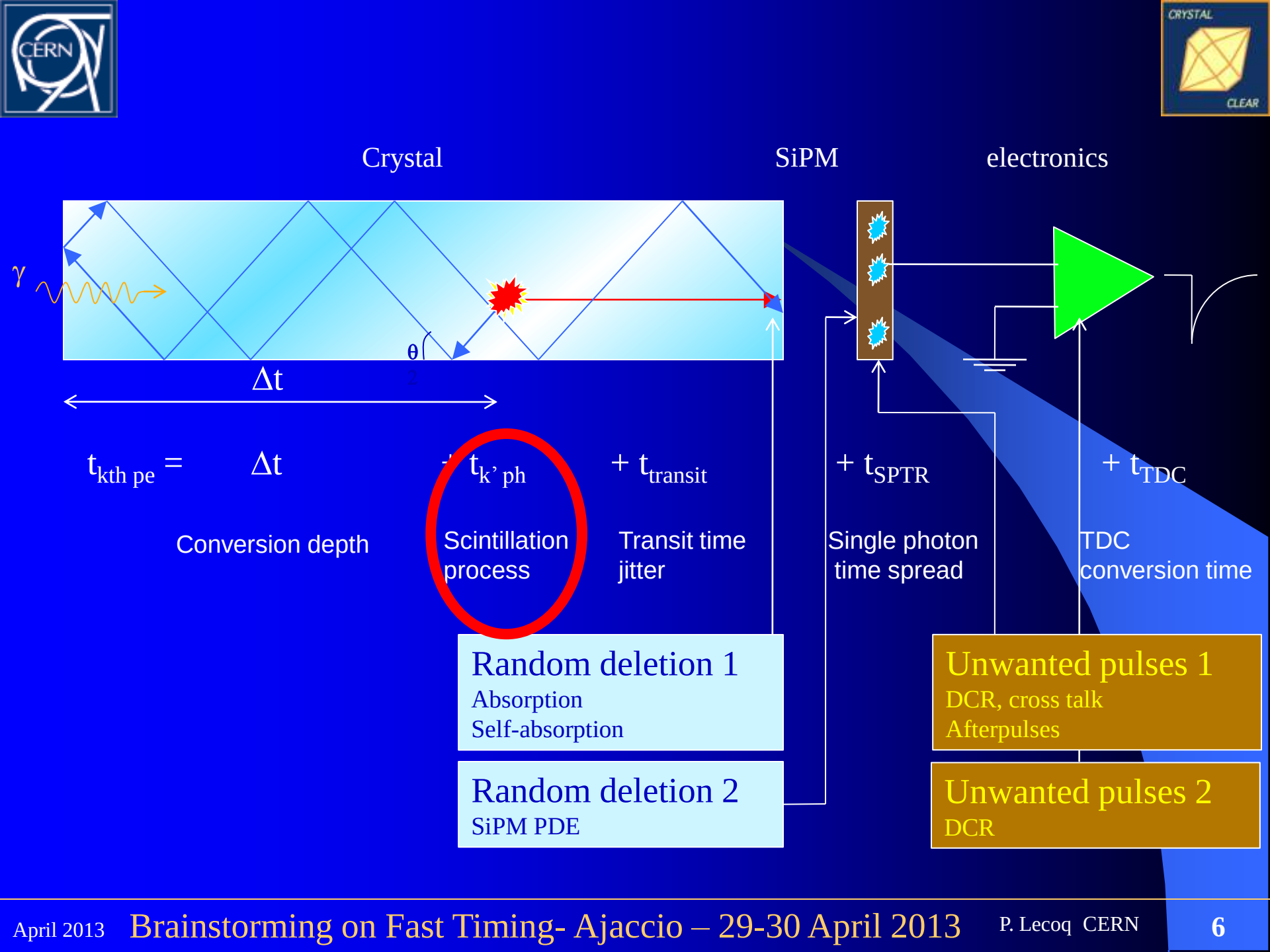
Crystal
SiPM
electronics
γ
θ
Δt
$t_{kth\ pe}$ = Δt + $t_{k'\ ph}$ + $t_{transit}$ + t_{SPTR} + t_{TDC}
Conversion depth
Scintillation process
Transit time jitter
Single photon time spread
TDC conversion time
Random deletion 1
Absorption
Self-absorption
Random deletion 2
SiPM PDE
Unwanted pulses 1
DCR, cross talk
Afterpulses
Unwanted pulses 2
DCR

Two types of decays for fast timing

- 100-200 photons within first 10 ps – 2 scenarios

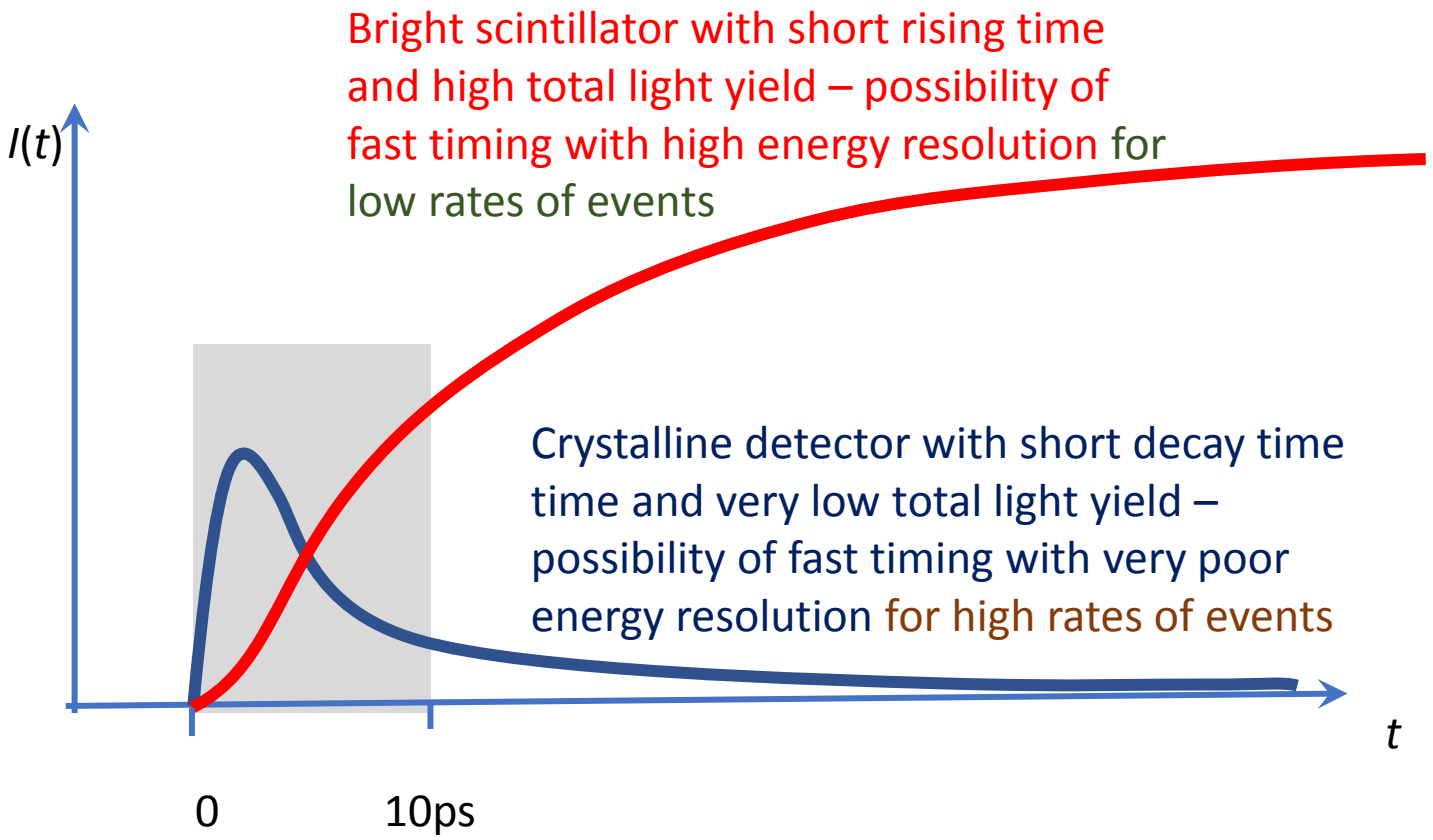

General description of stages of energy relaxation in scintillators

Types of emission in scintillating crystals and delay between energy deposit and photon emission

- Excitonic emission (STE, excitations of anion complexes)
- Emission of activators (Ce, Pr, …)
- Crossluminescence
- Intraband hot luminescence
- Cherenkov radiation

Scheme of relaxation of electronic excitations in crystals with “simple” energy structure

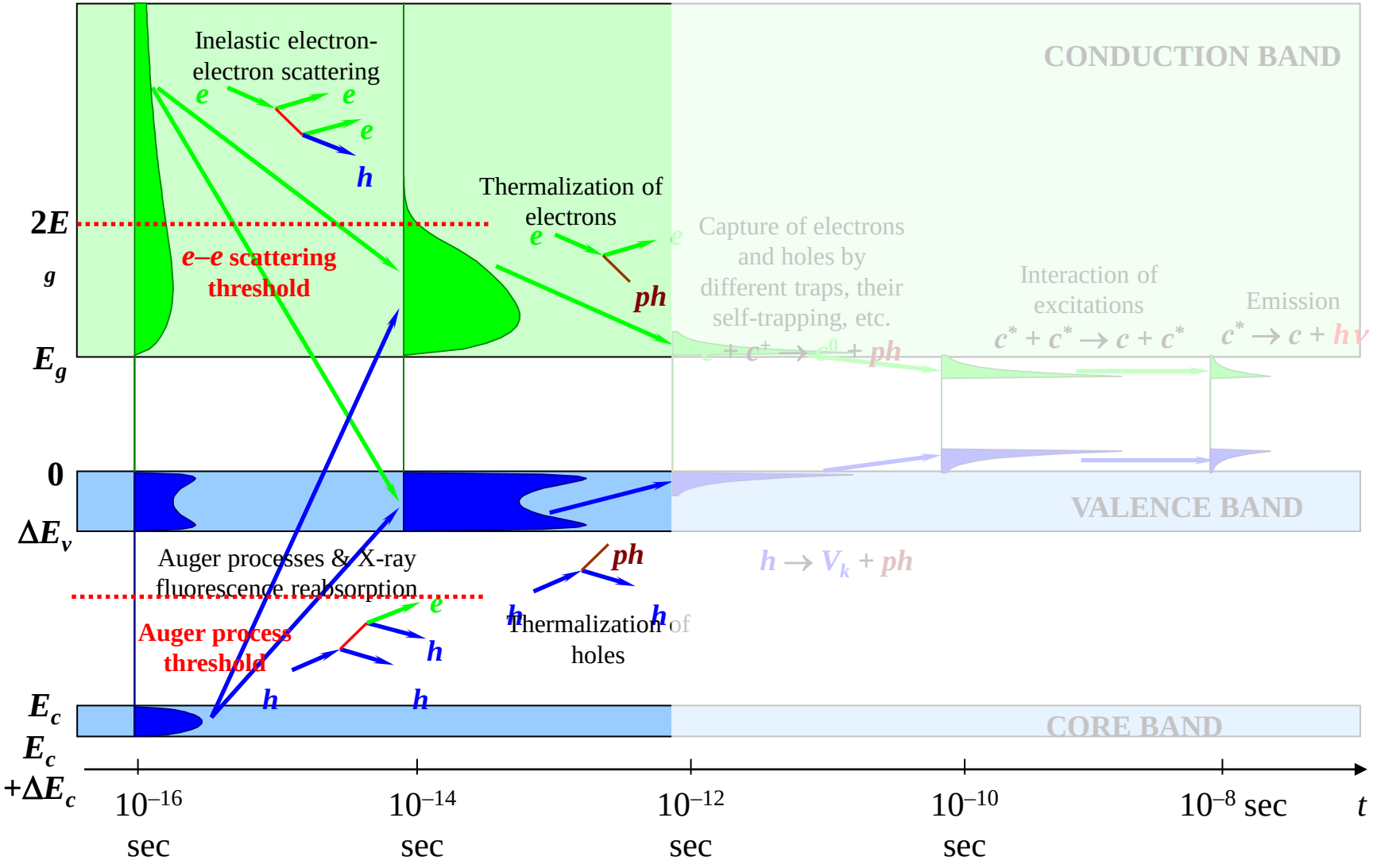

An example of Monte-Carlo simulation of spatial distribution of electrons and holes in CsI before thermalization

11387 e-h pairs

$E_{eh}=1.46E_g$

First scattering of primary 100 keV photoelectron

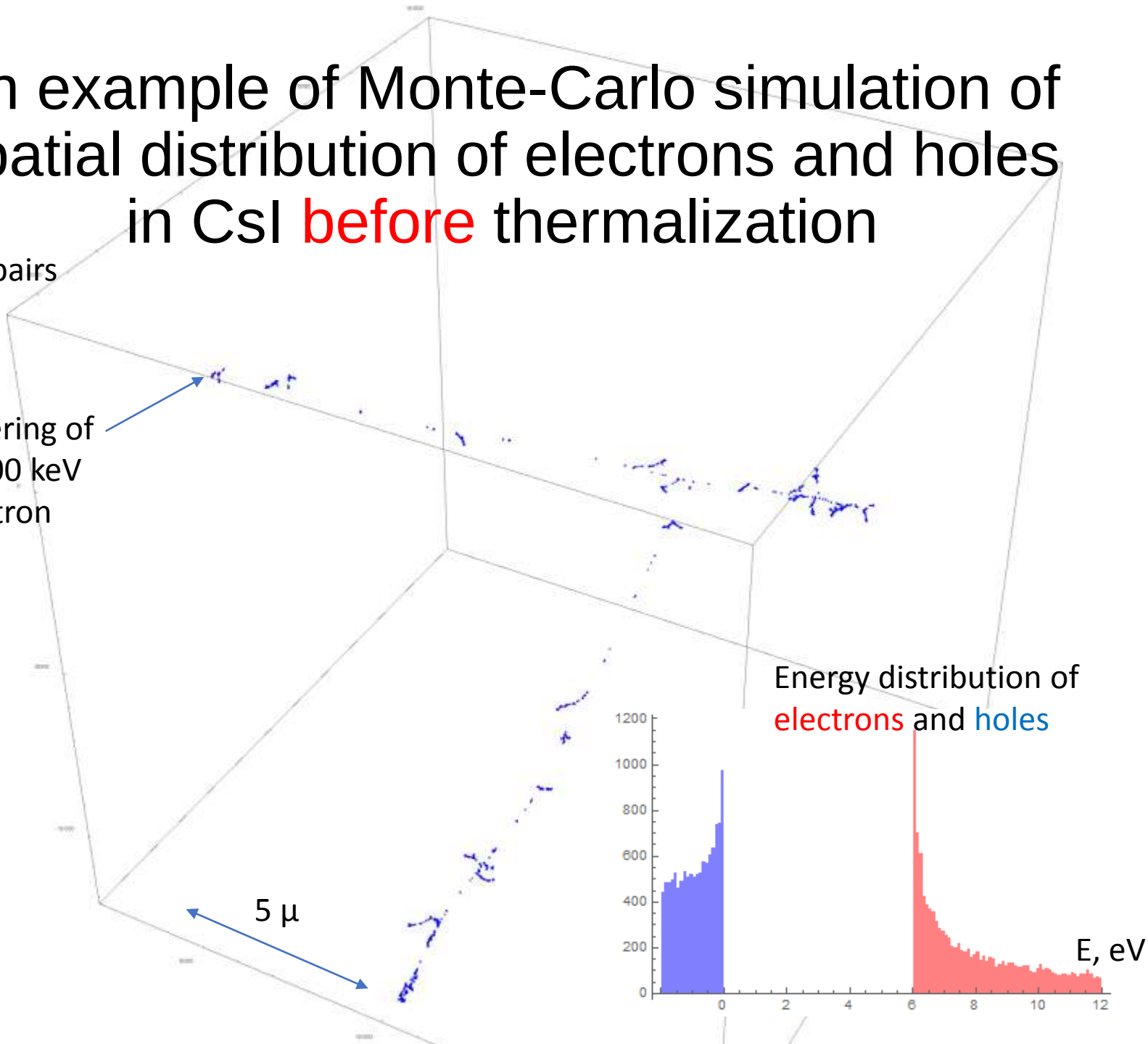

Energy distribution of electrons and holes

Thermalization length and time for different phonon parameters (analytical for parabolic bands)

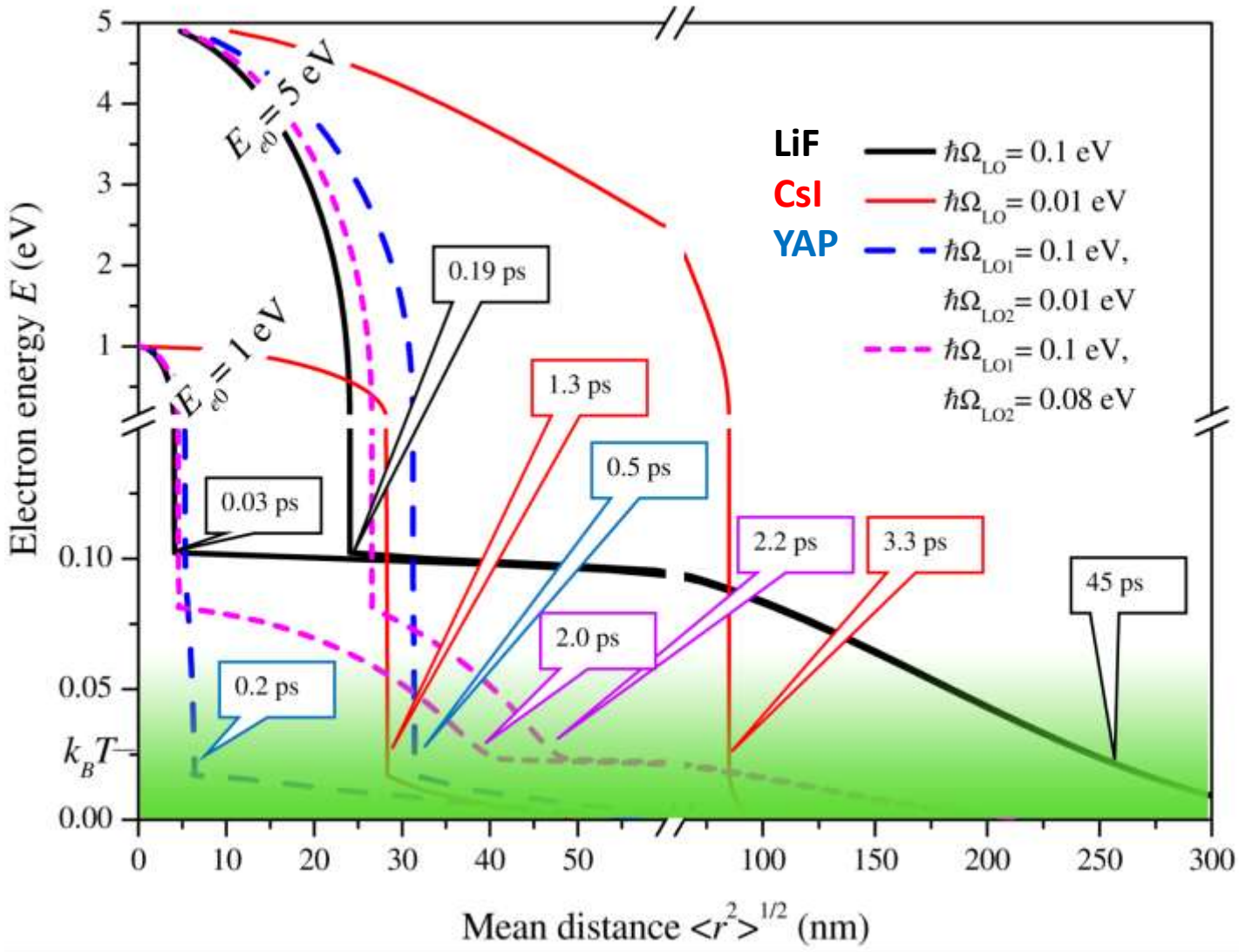

R. Kirkin, V.V. Mikhailin, and A.N. Vasil'ev, *Recombination of correlated electron-hole pairs with account of hot capture with emission of optical phonons*, IEEE Transactions on Nuclear Science, vol. 59, issue 5, pp. 2057-2064 (2012)

An example … of spatial distr… les in Cs…

11387 e-h pairs
$E_{eh}=1.46E_g$

First scattering of primary 100 keV photoelectron

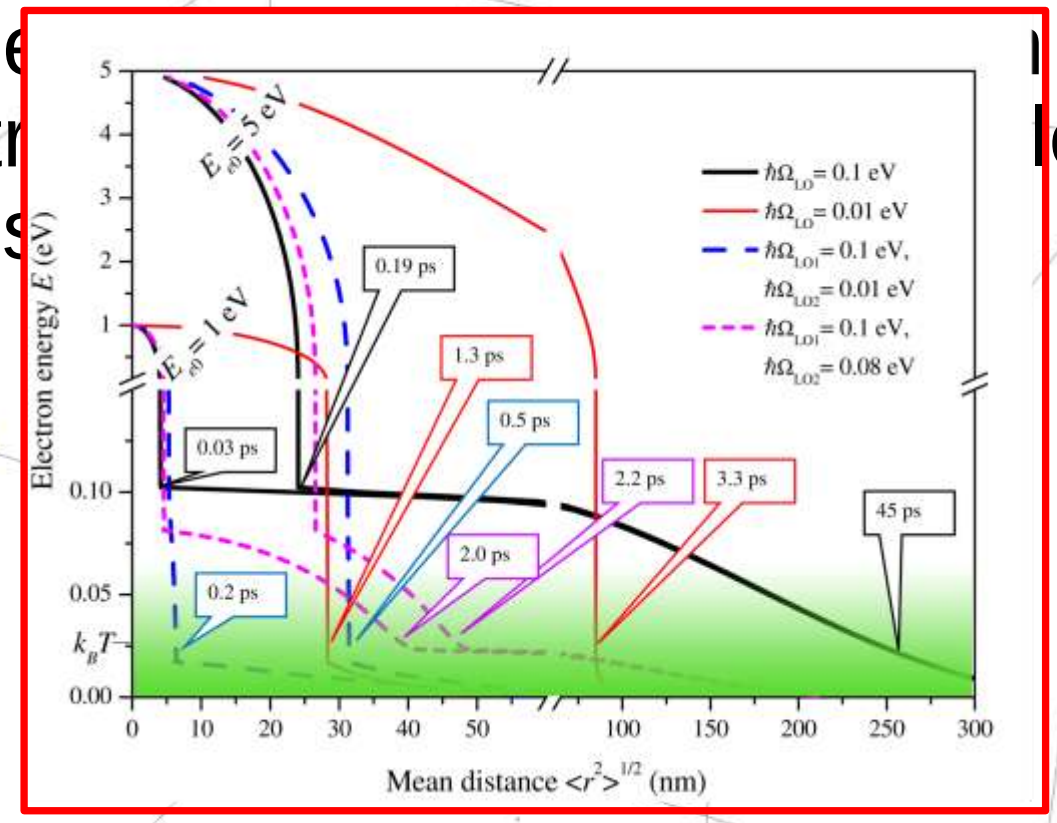

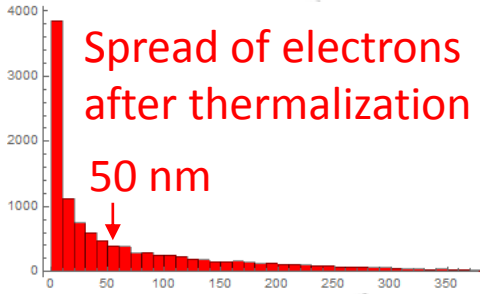

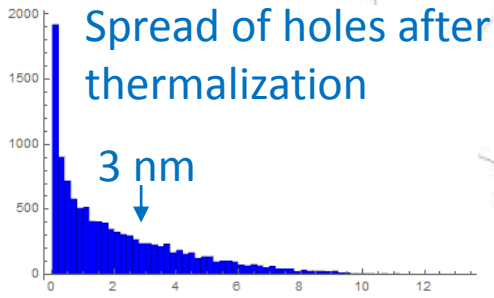

5 μ

Energy distribution of electrons and holes

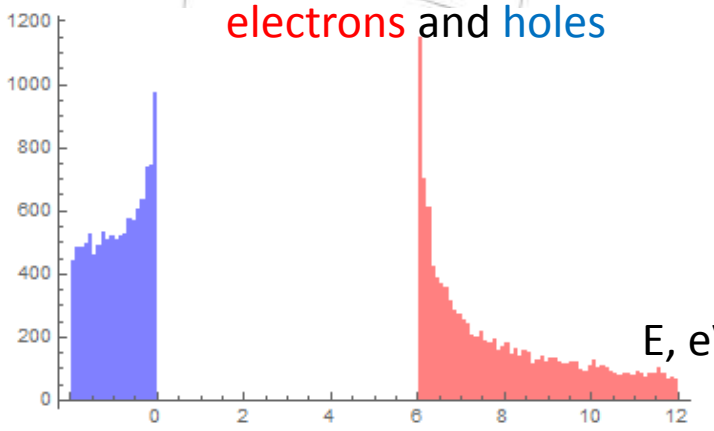

An example of Monte-Carlo simulation of spatial distribution of electrons and holes in CsI after thermalization

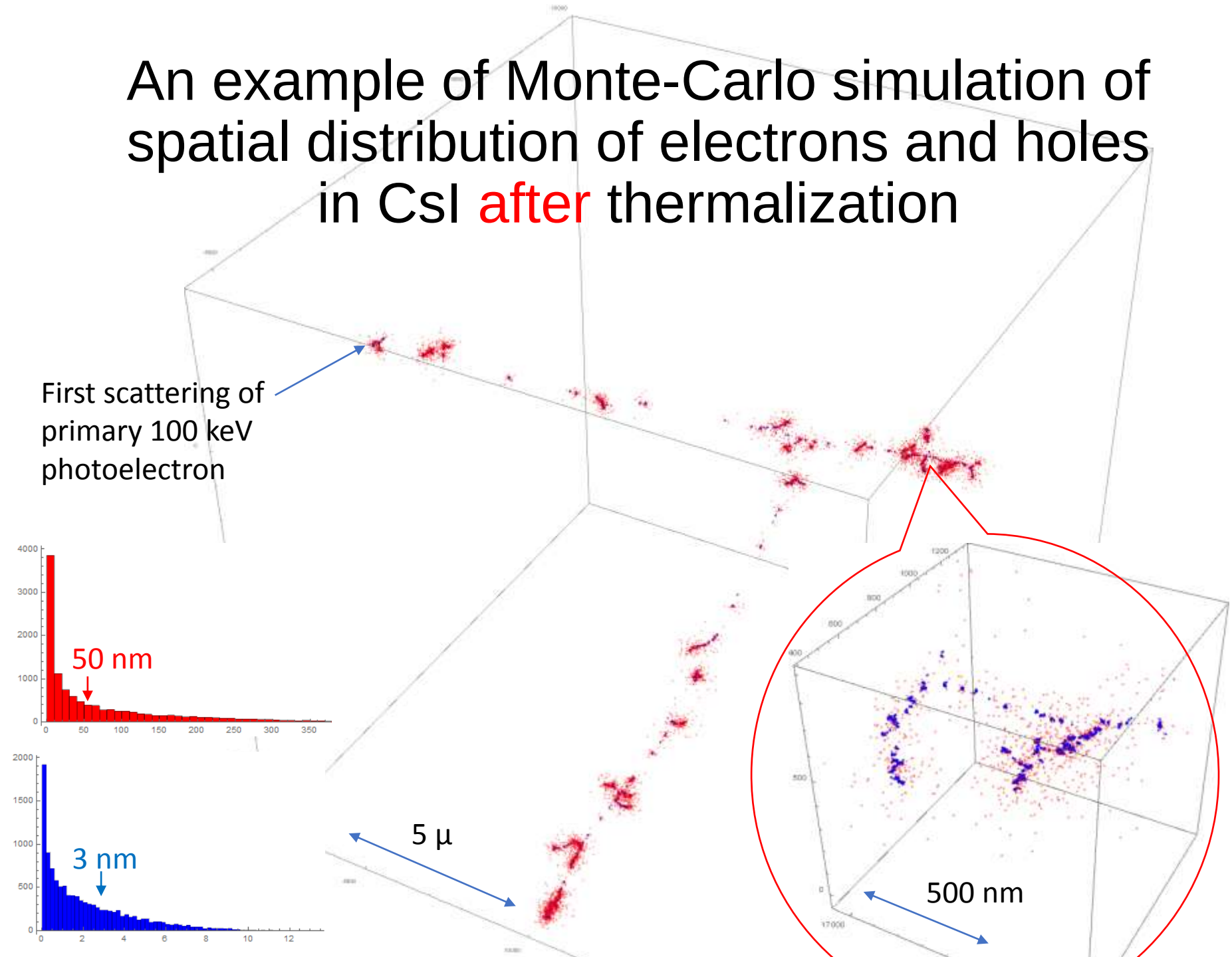

Timing properties of IBL and CL

Intra-band luminescence for complex band structure (schemas)

Crystals with dip in the conduction or valence band

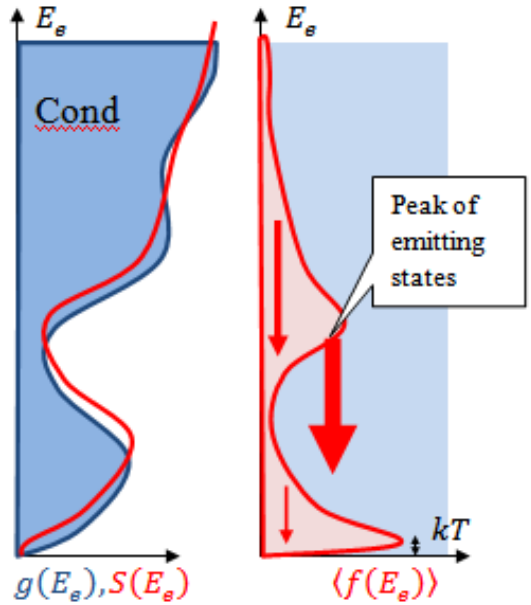

$\tau_{em} \approx 10^{-12}$ sec

Crystals with gap in the conduction or valence band

$\tau_{em} \approx 10^{-10}$ sec

Crossluminescent crystals (wide gap in valence band)

$\tau_{em} \approx 10^{-9}$ sec

The gaps within the conduction bands occur in crystals with *d*-electrons (e.g. Cond2 arises from *s*-electrons, whereas Cond1 – from *d*-electrons: CeF_3, crystals with WO_4 and MoO_4 groups, etc.) and in spin-orbit split valence bands

Thermalization length and time for different phonon parameters (analytical for parabolic bands)

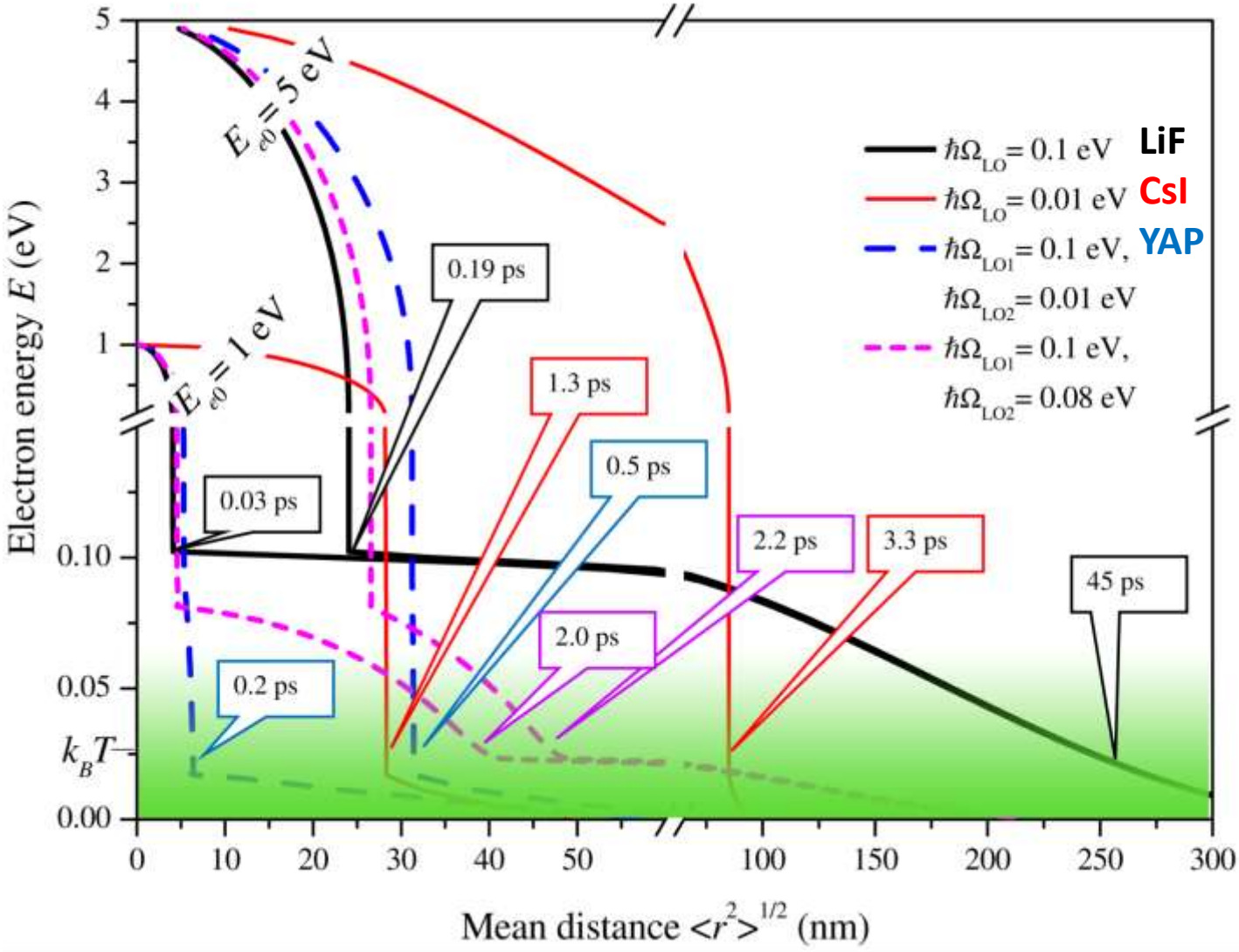

Radiation time depends on energy of emitted photons

$$\tau_r \approx 1\ \text{ns} \left(\frac{5\ \text{eV}}{\hbar\omega_{emission}} \right)^2$$

$\tau_r \approx 1$ ns for $\hbar\omega_{emission} = 5$ eV

$\tau_r \approx 6.2$ ns for $\hbar\omega_{emission} = 2$ eV

$\tau_r \approx 25$ ns for $\hbar\omega_{emission} = 1$ eV

IBL yield

$$\eta = \frac{\tau_{therm}}{\tau_r} = 10^{-4} \div 10^{-3}$$

R. Kirkin, V.V. Mikhailin, and A.N. Vasil'ev, *Recombination of correlated electron-hole pairs with account of hot capture with emission of optical phonons*, IEEE Transactions on Nuclear Science, vol. 59, issue 5, pp. 2057-2064 (2012)

Estimation of spectrum of IBL

Russian Physics Journal, Vol. 40, No. 11, 1997

TWO TYPES OF FUNDAMENTAL LUMINESCENCE OF IONIZATION-PASSIVE ELECTRONS AND HOLES IN OPTICAL DIELECTRICS — INTRABAND-ELECTRON AND INTERBAND-HOLE LUMINESCENCE (THEORETICAL CALCULATION AND COMPARISON WITH EXPERIMENT)

D. I. Vaisburd and S. V. Kharitonova

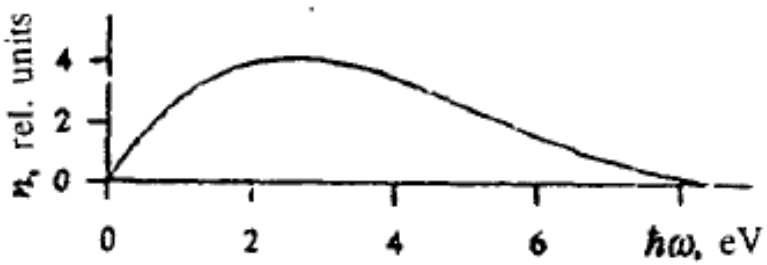

Fig. 17

Fig. 17. Calculated spectrum of intraband electron luminescence of CsI excited by a pulsed electron beam.

e-IBL spectrum and decay (continuous distribution of branches)

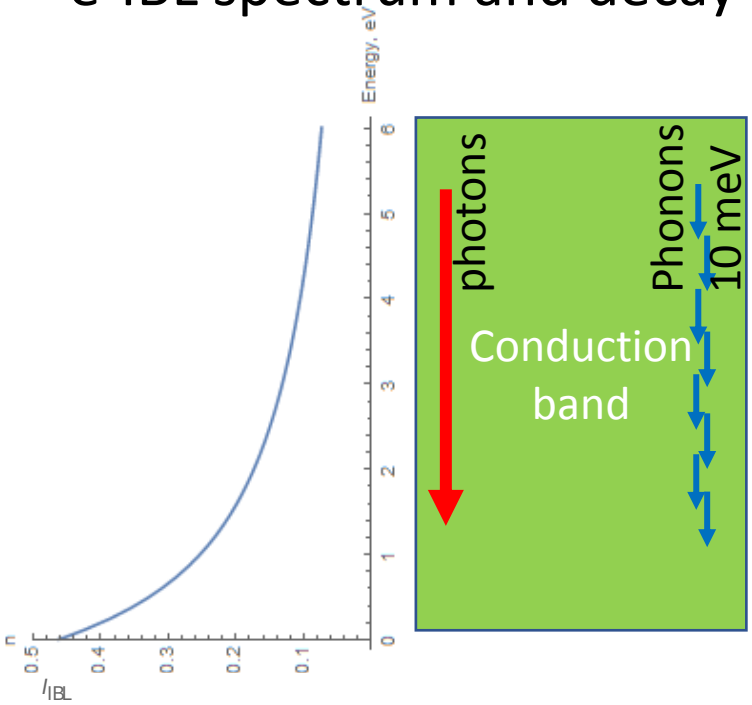

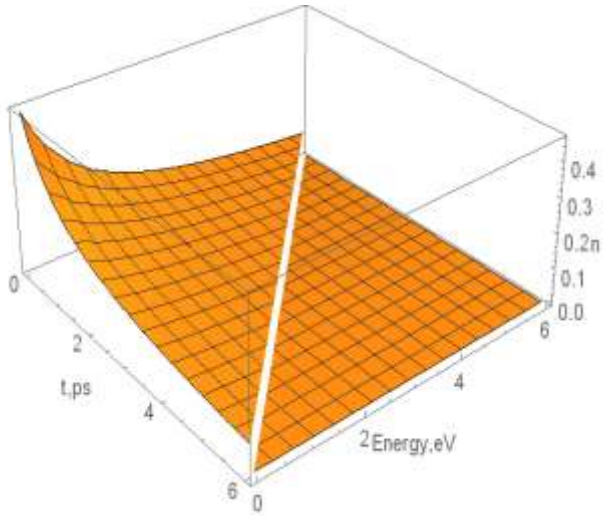

Evolution of electron energy distribution in time

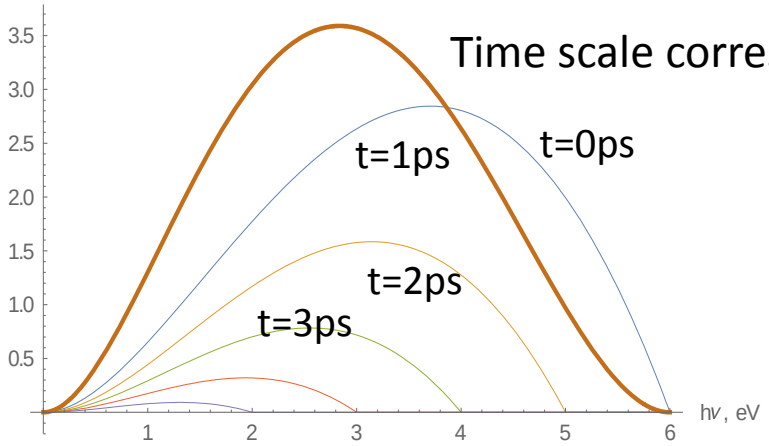

Evolution of e-IBL spectrum in time

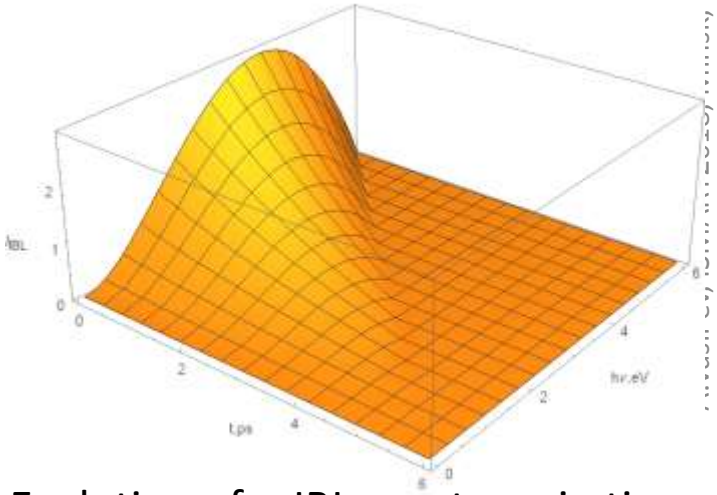

Evolution of e-IBL spectrum in time

e-IBL spectrum and decay (continuous distribution of branches)

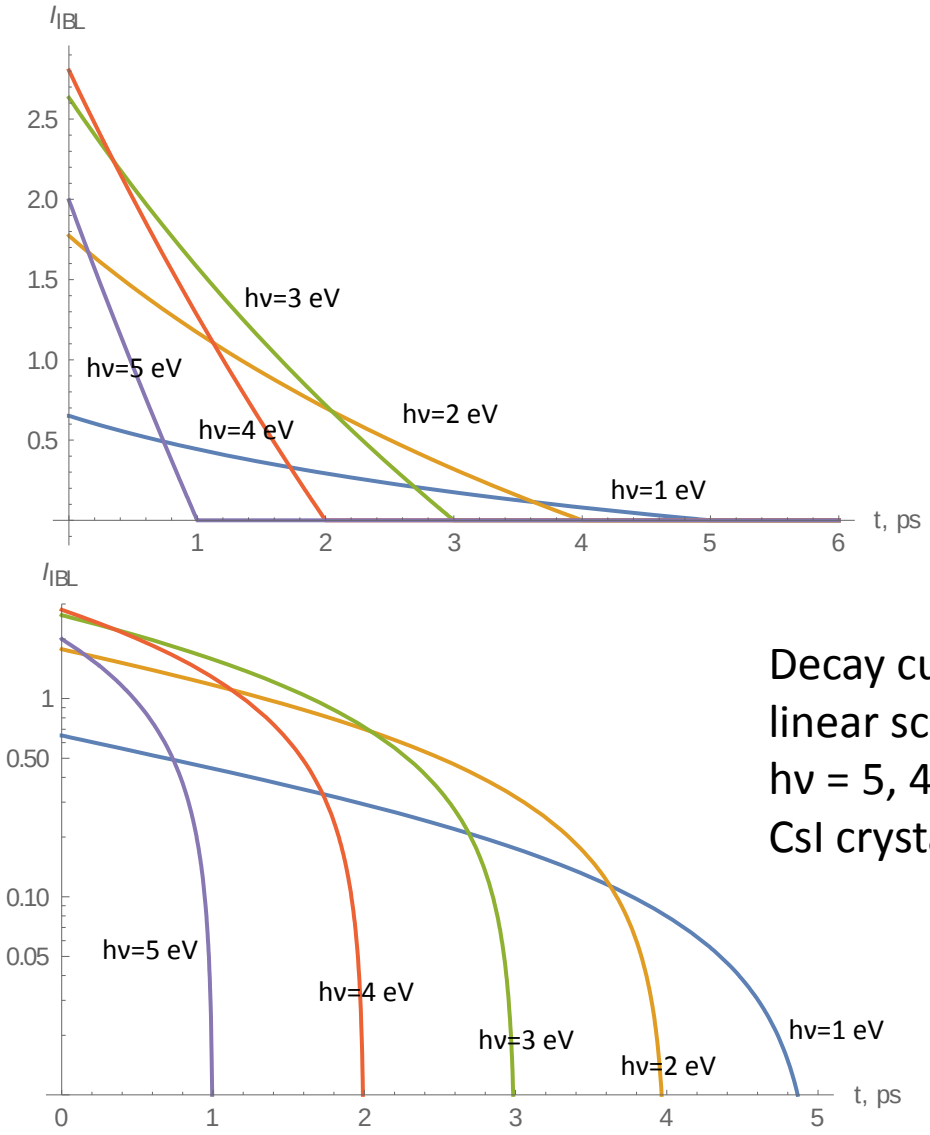

Decay curves for different photon energies: top – linear scale, bottom – semilogarithmic scale for hν = 5, 4, 3, 2, 1 eV. Time scale corresponds to CsI crystal (phonon energy 10 meV)

e-IBL emission spectrum for the model of Multiple Parabolic Band approximation (nearly free electrons) - dependence on electron mass (number of branches up to E_g kinetic energy)

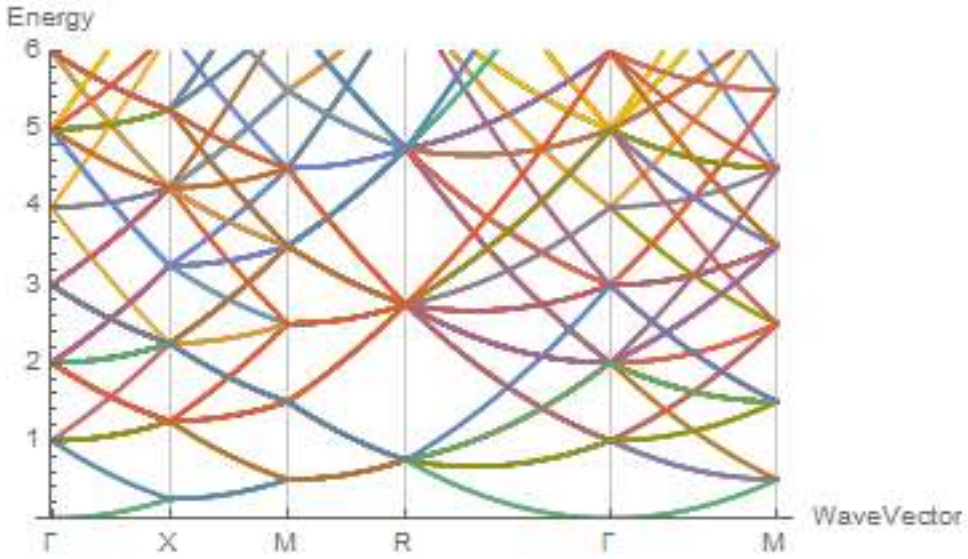

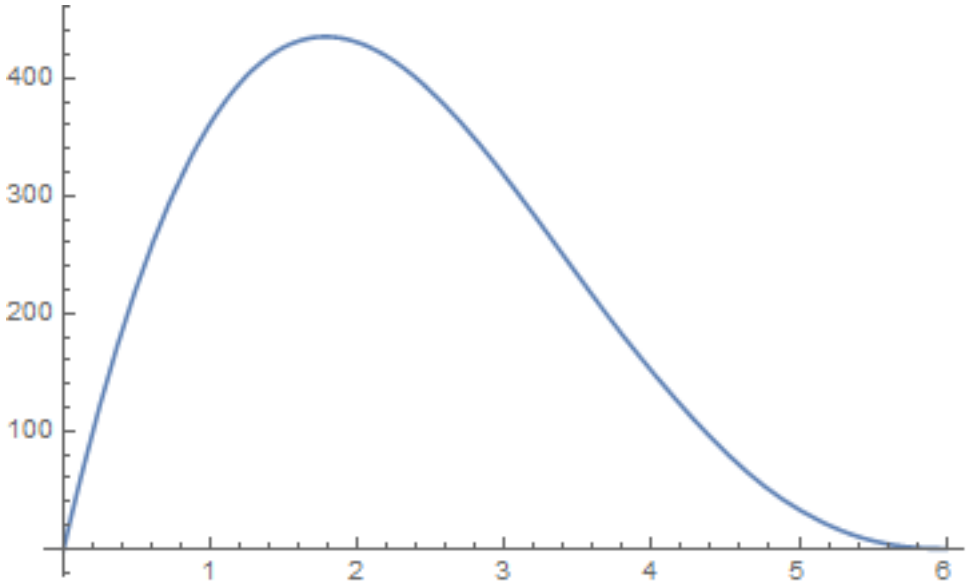

e-IBL emission spectrum for the model of Multiple Parabolic Band approximation (nearly free electrons) - dependence on electron mass (number of branches up to E_g kinetic energy)

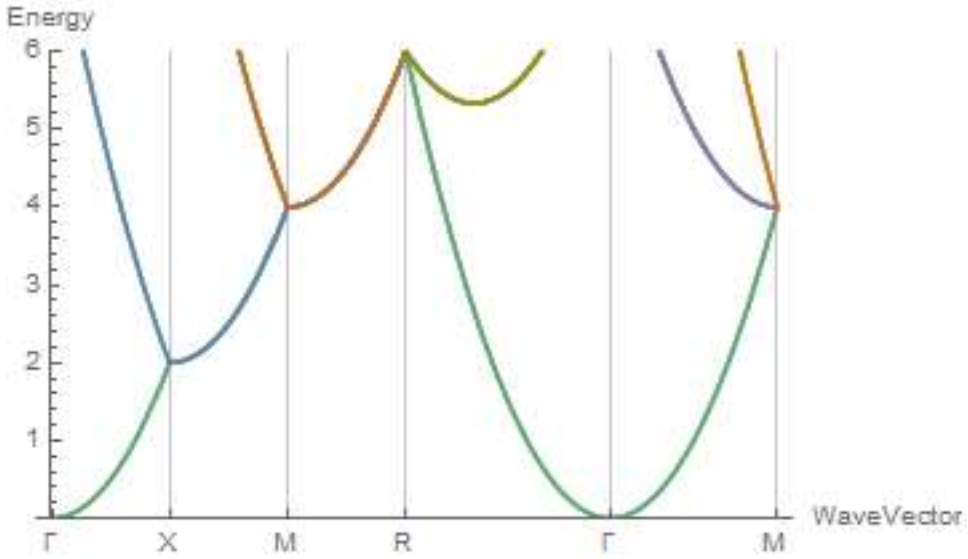

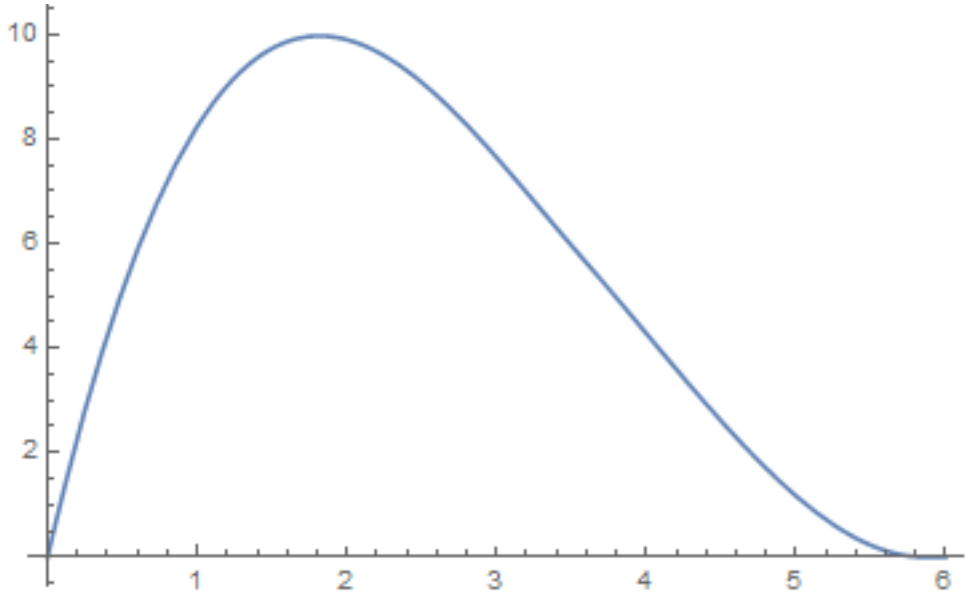

Second order processes in IBL

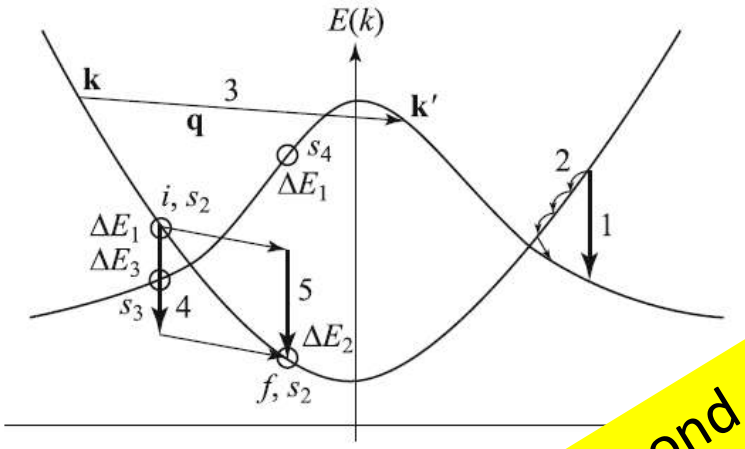

Fig. 1. Schematic diagram of relax
conduction band of an insulato

$\Delta E_1 = E_i(\mathbf{k}_i) - [E_{s1}(\mathbf{k}_i)$
$\Delta E_2 = E_i(\mathbf{k}_i) - [E_{s}$
$\Delta E_3 = E_i(\mathbf{k}_i) -$
$\Delta E_4 = E_i(\mathbf{k}$ $f) - E_{s4}(\mathbf{k}_f) + \hbar\omega.$

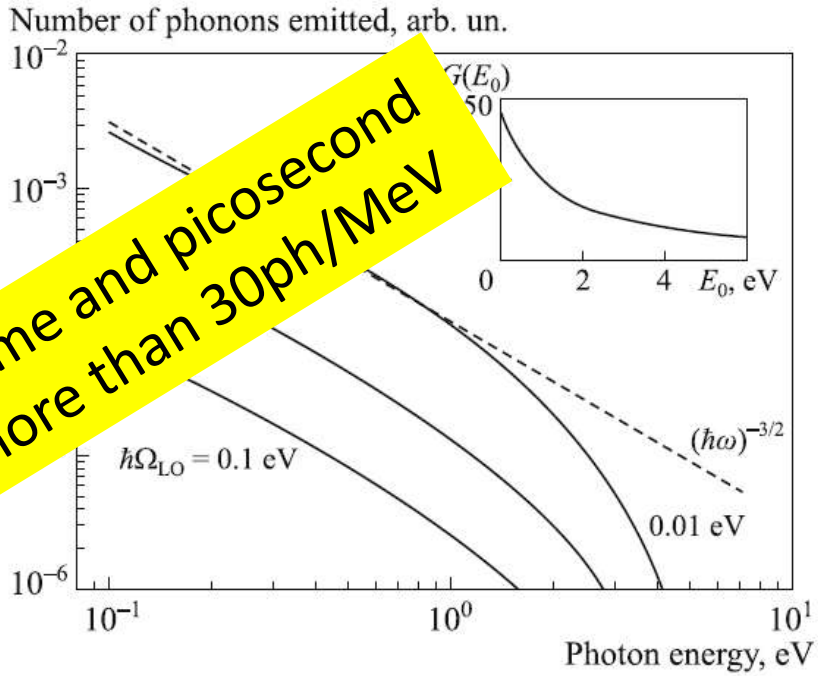

Fig. 3. Spectral distribution of the number of phonons emitted by secondary electrons produced by an ionizing particle for different phonon energies $\hbar\Omega_{LO}$ (labeled at the curves). The dashed lines correspond to the $(\hbar\omega)^{-1/2}$ trend. The inset shows the distribution of kinetic energies of secondary electrons used for this calculation and corresponding to Eq. (18).

IBL has subpicosecond rise time and picosecond decay, but it's yield is not more than 30ph/MeV

A.Vasil'ev, R.Kirkin, Physics of Wave Phenomena, 2015, 23 (2015) 186-191

Intra-band luminescence for complex band structure (schemas)

Crystals with dip in the conduction or valence band

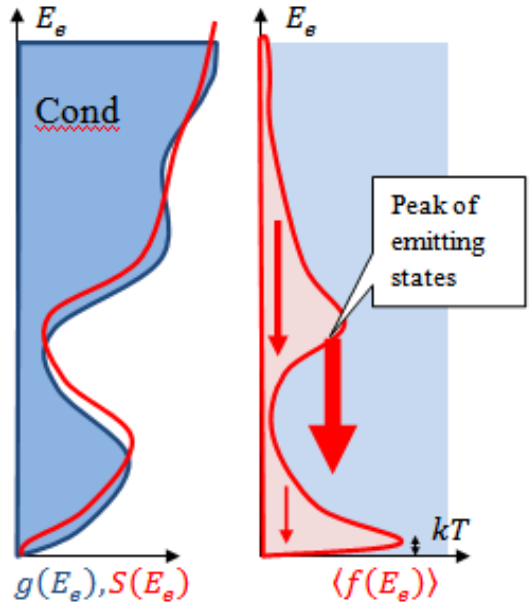

$\tau_{em} \approx 10^{-12}$ sec

Crystals with gap in the conduction or valence band

$\tau_{em} \approx 10^{-10}$ sec

Crossluminescent crystals (wide gap in valence band)

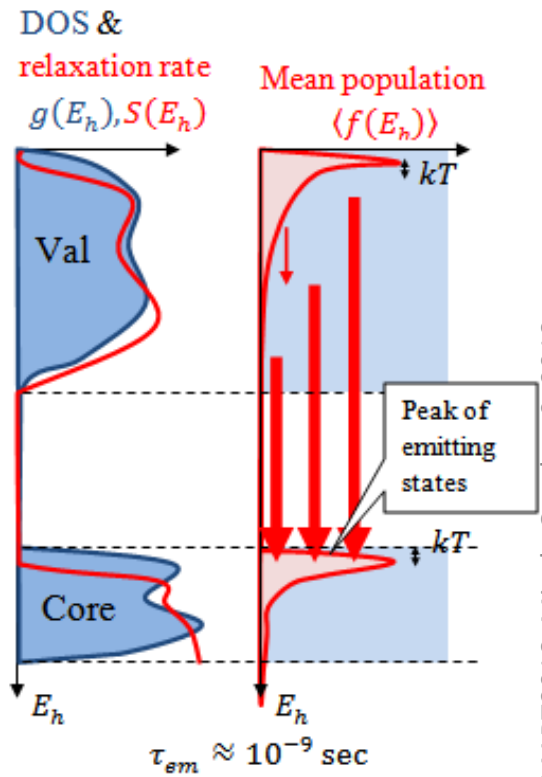

$\tau_{em} \approx 10^{-9}$ sec

The gaps within the conduction bands occur in crystals with *d*-electrons (e.g. Cond2 arises from *s*-electrons, whereas Cond1 – from *d*-electrons: CeF_3, crystals with WO_4 and MoO_4 groups, etc.) and in spin-orbit split valence bands

Crossluminescence (CL)

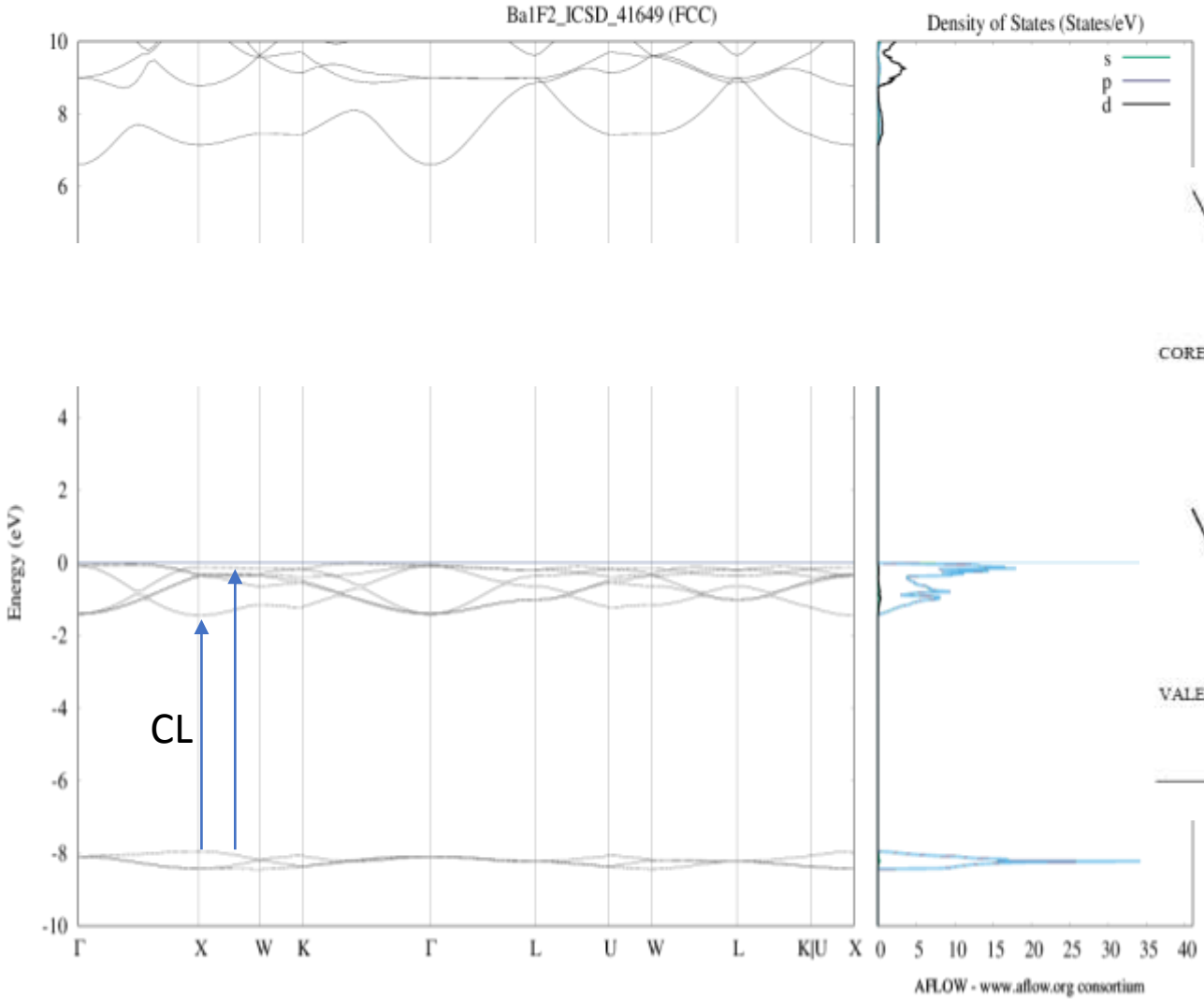

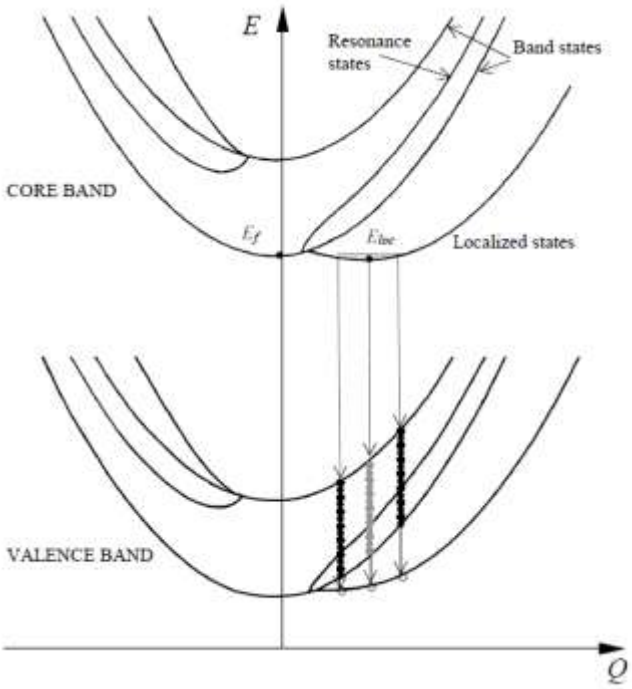

Self-trapping of core holes modifies the valence band states

BaF_2 band structure (AFLOWLib.org)

Energy distribution of the population of electrons and holes after cascade (Monte Carlo)

How many electrons and holes with high energy could be created after cascade stage?

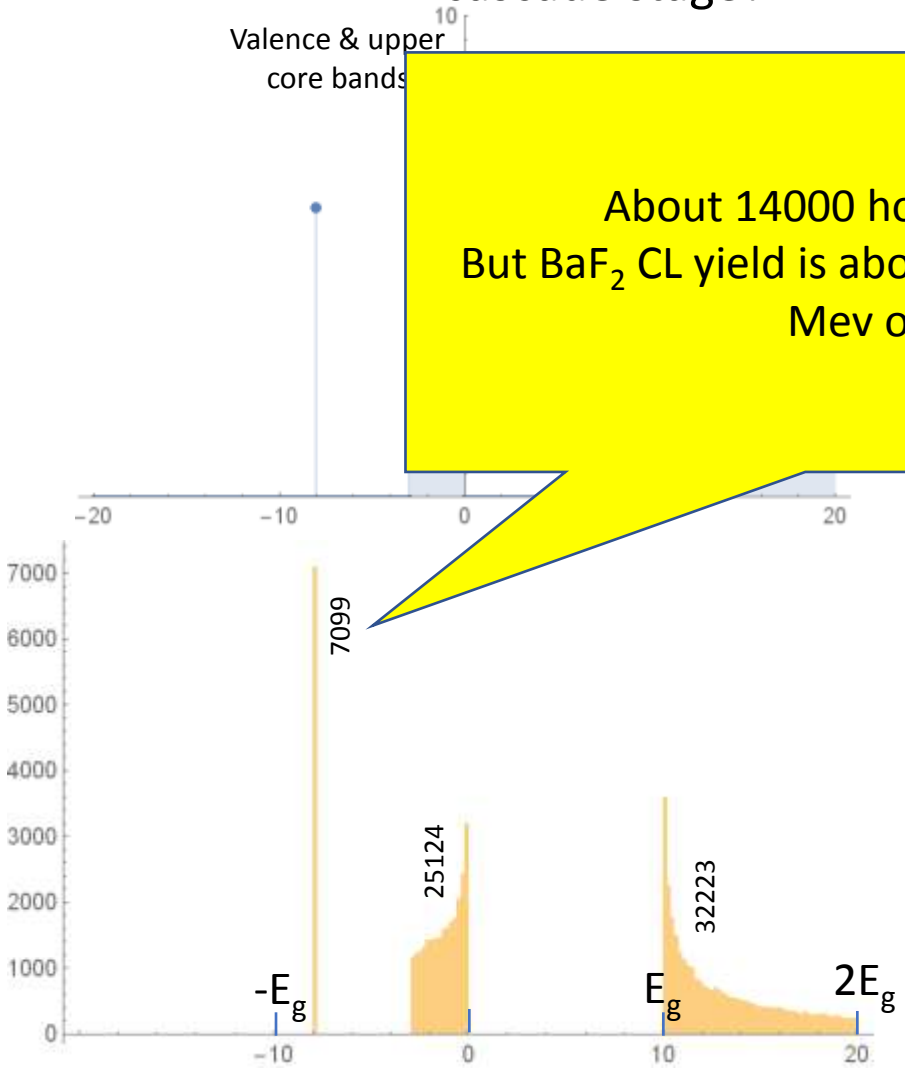

About 14000 holes per MeV!
But BaF_2 CL yield is about 2000 photons per Mev only!

Monte-Carlo simulation of distribution of electrons and holes (bottom panel) for DOS presented in upper panel (case of BaF_2). Distribution is calculated for 511 keV.

Quenching of BaF_2 crossluminescence vs excitation energy

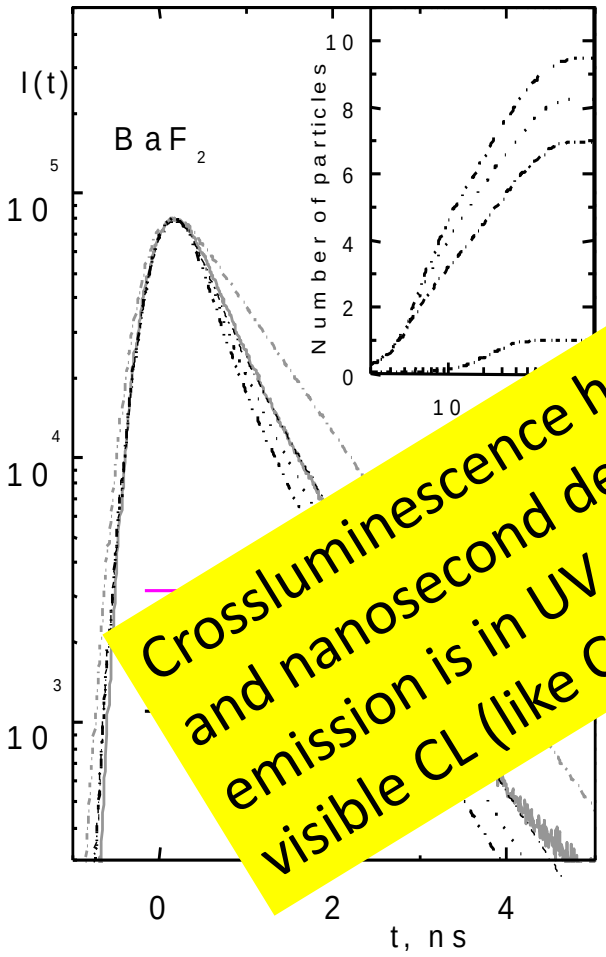

Crossluminescence has subpicosecond rise time and nanosecond decay, its yield is moderate, but emission is in UV and VUV. Binary crystals with visible CL (like CsF) are very hygroscopic.

Dependen luminescence on the e in terms of th bor excitations ning of the

BaF_2 crossluminescence decay kinetics ation by photons with different energy corresponding distribution of neighbor rations (in the inset) [Glukhov R.A., Kamada M., Kubota S., Nakamura E., Ohara S., Terekhin M. A., Vasil'ev A. N., Proc. Int. Conf. on Inorganic Scintillators and Their Applications, SCINT95, Delft University Press, The Netherlands (1996) 204].

Intra-band luminescence for complex band structure (schemas)

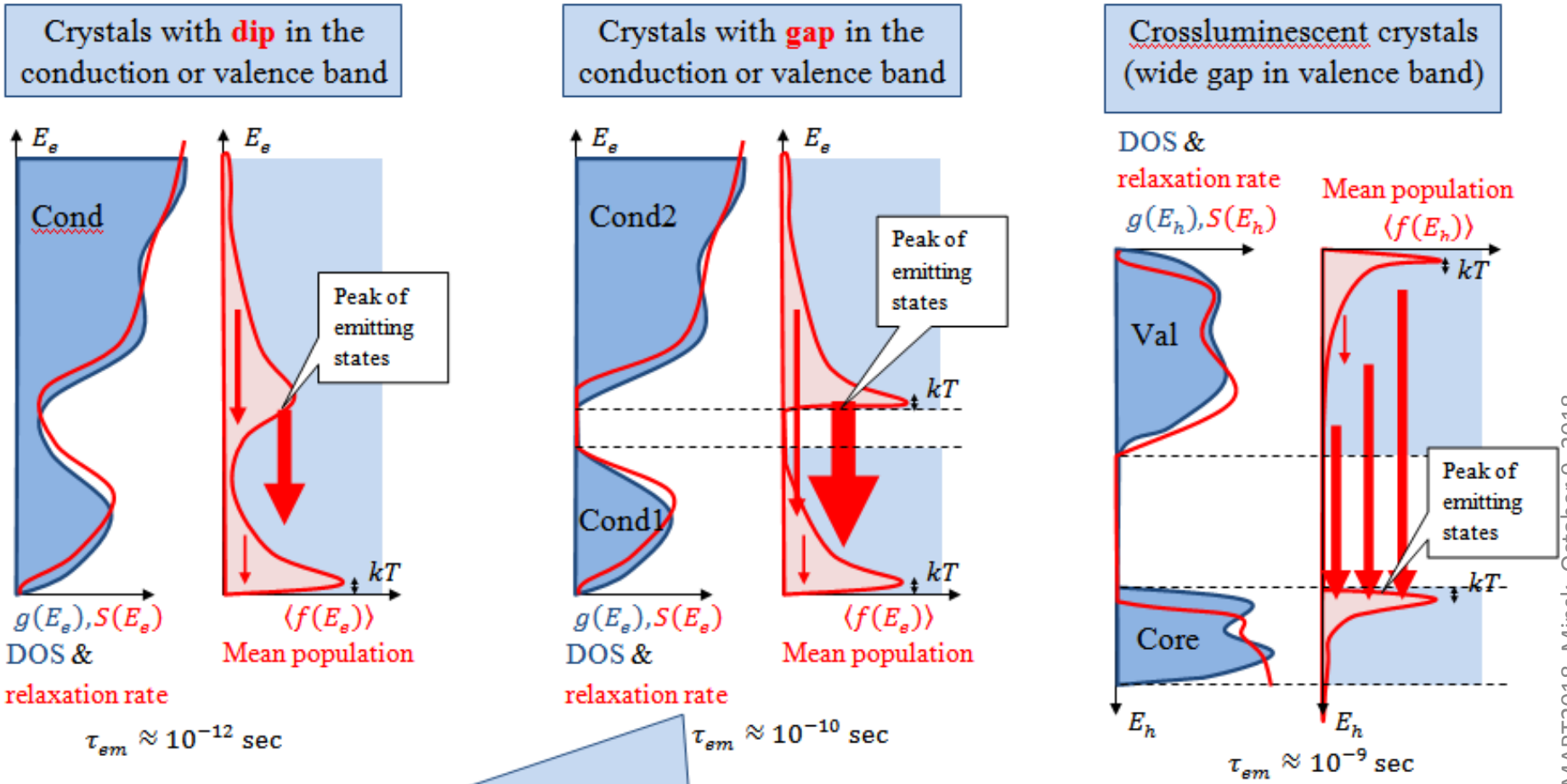

The gaps within the conduction bands occur in crystals with *d*-electrons (e.g. Cond2 arises from *s*-electrons, whereas Cond1 – from *d*-electrons: CeF_3, crystals with WO_4 and MoO_4 groups, etc.) and in spin-orbit split valence bands

See S.Omelkov talk

A.Vasil'ev, ISMART2018, Minsk, October 9, 2018

Timing properties of recombination luminescence

Excitonic energy transfer to Ce^{3+}

- Three (four) sequential processes:

1. bi-molecular e+h→FE
2. monomolecular FE →STE
3. bi-molecular STE+Ce^{3+} →Ce^{3+*}

- or

3. STE+Ce^{3+} →Ce^{4+}+e
4. Ce^{4+}+e →Ce^{3+*}

After convolution of rise functions of these processes and averaging over distribution of concentrations rise time becomes multi-component

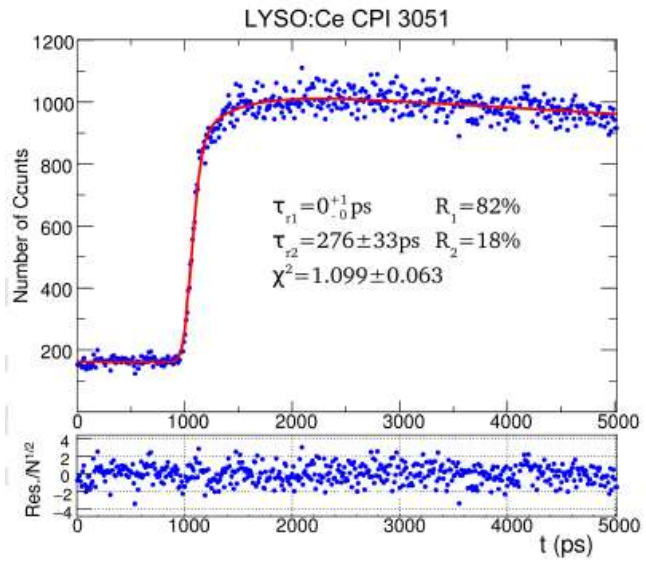

S. Gundacker, R.M. Turtos, E. Auffray, P. Lecoq, Precise rise and decay time measurements of inorganic scintillators by means of X-ray and 511 keV excitation, Nuclear Inst. and Methods in Physics Research, A (2018), https://doi.org/10.1016/j.nima.2018.02.074

Types of energy transfer to emission centers and time resolution

Decay time τ_{em}=40ns

Yield N_{em}=40000 photons

Detection threshold N_{th}=20

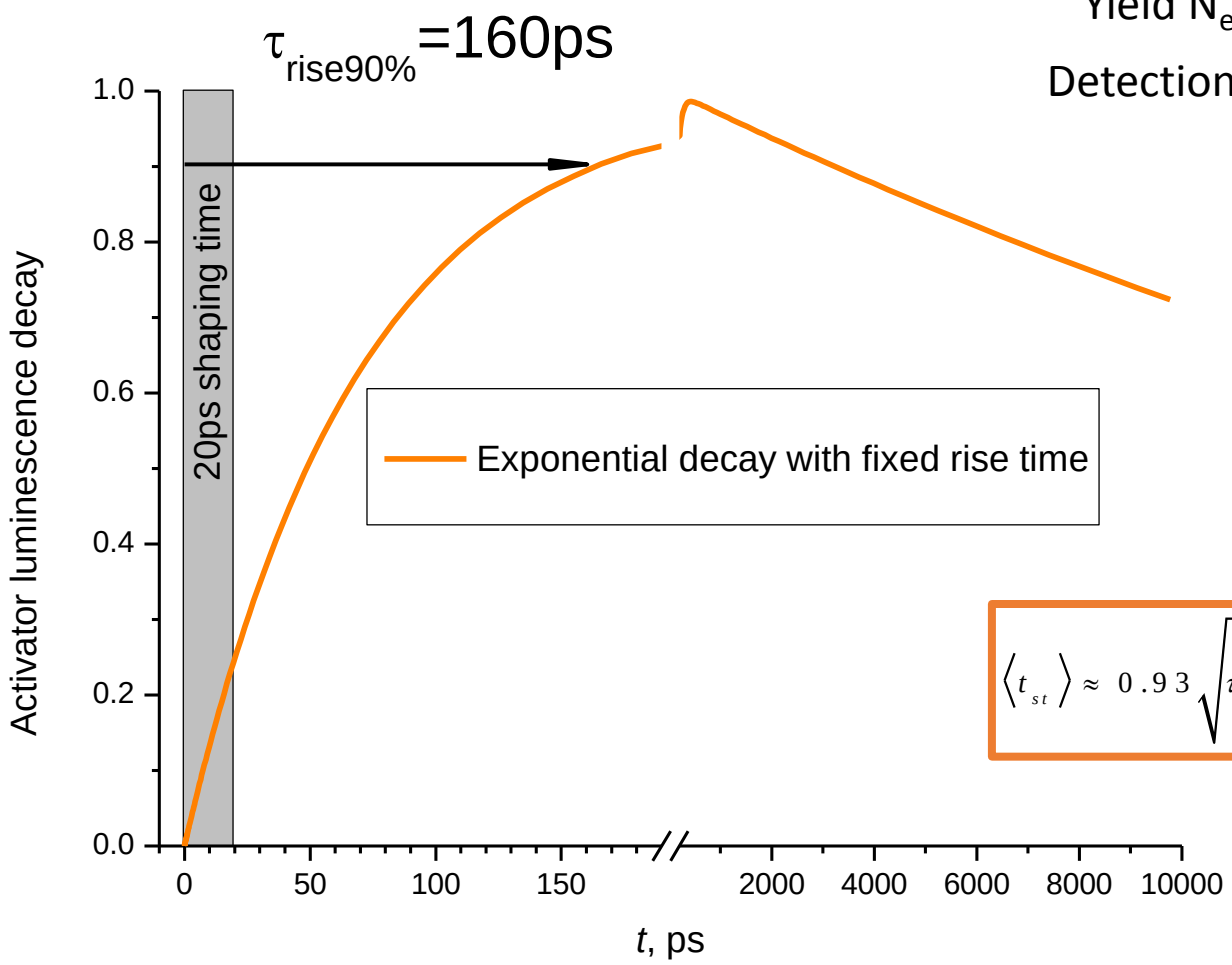

$$\langle t_{st} \rangle \approx 0.93 \sqrt{\tau_{em}\,\tau_{rise90\%}\,\frac{N_{th}}{N_{em}}} = 53\,\text{ps}$$

Types of energy transfer to emission centers and time resolution

Decay time τ_{em}=40ns

Yield N_{em}=40000 photons

Detection threshold N_{th}=20

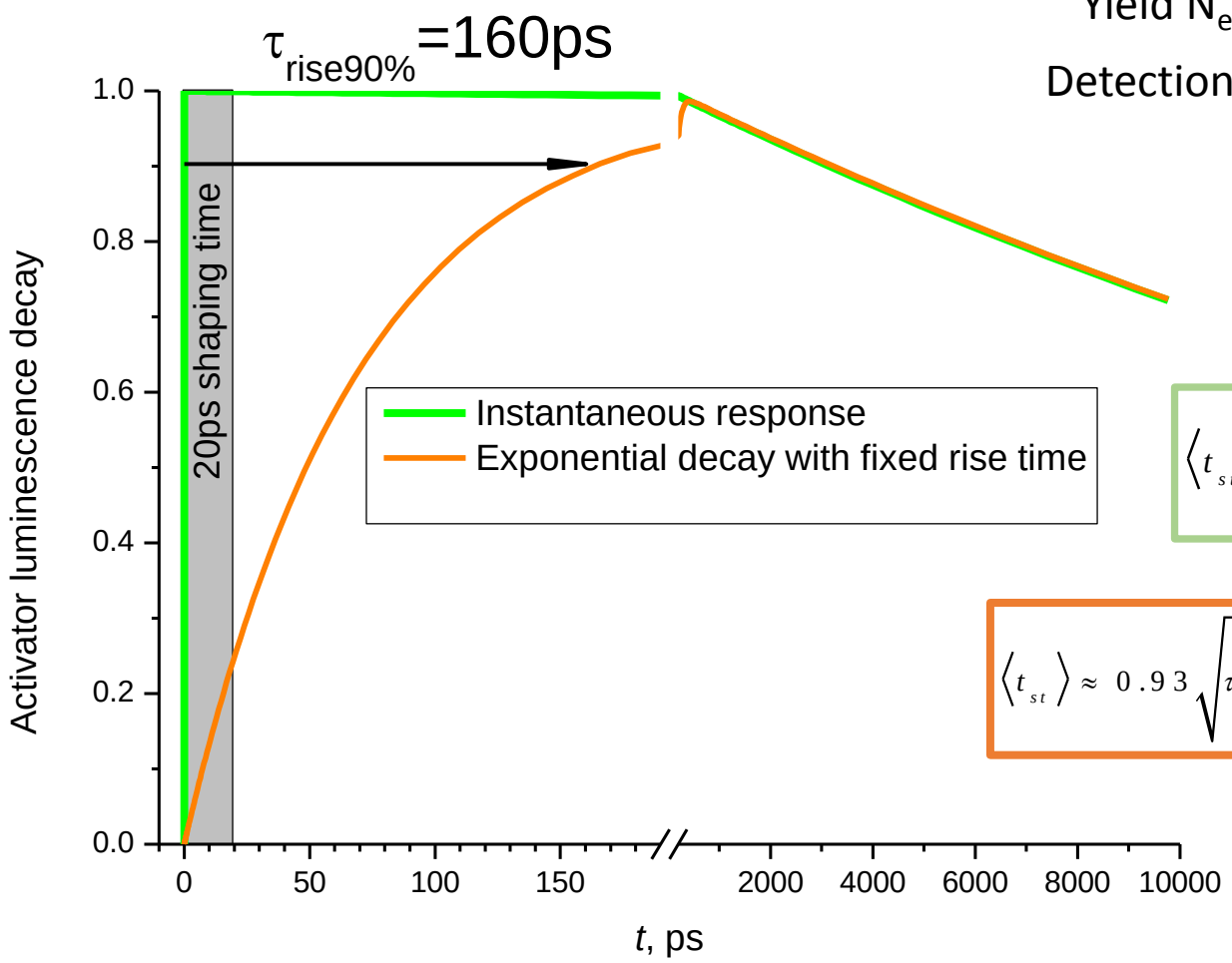

$$\langle t_{st} \rangle \approx \tau_{em} \frac{N_{th}}{N_{em}} = 20\,\text{ps}$$

$$\langle t_{st} \rangle \approx 0.93 \sqrt{\tau_{em} \tau_{rise90\%} \frac{N_{th}}{N_{em}}} = 53\,\text{ps}$$

Types of energy transfer to emission centers and time resolution

Decay time τ_{em}=40ns

Yield N_{em}=40000 photons

Detection threshold N_{th}=20

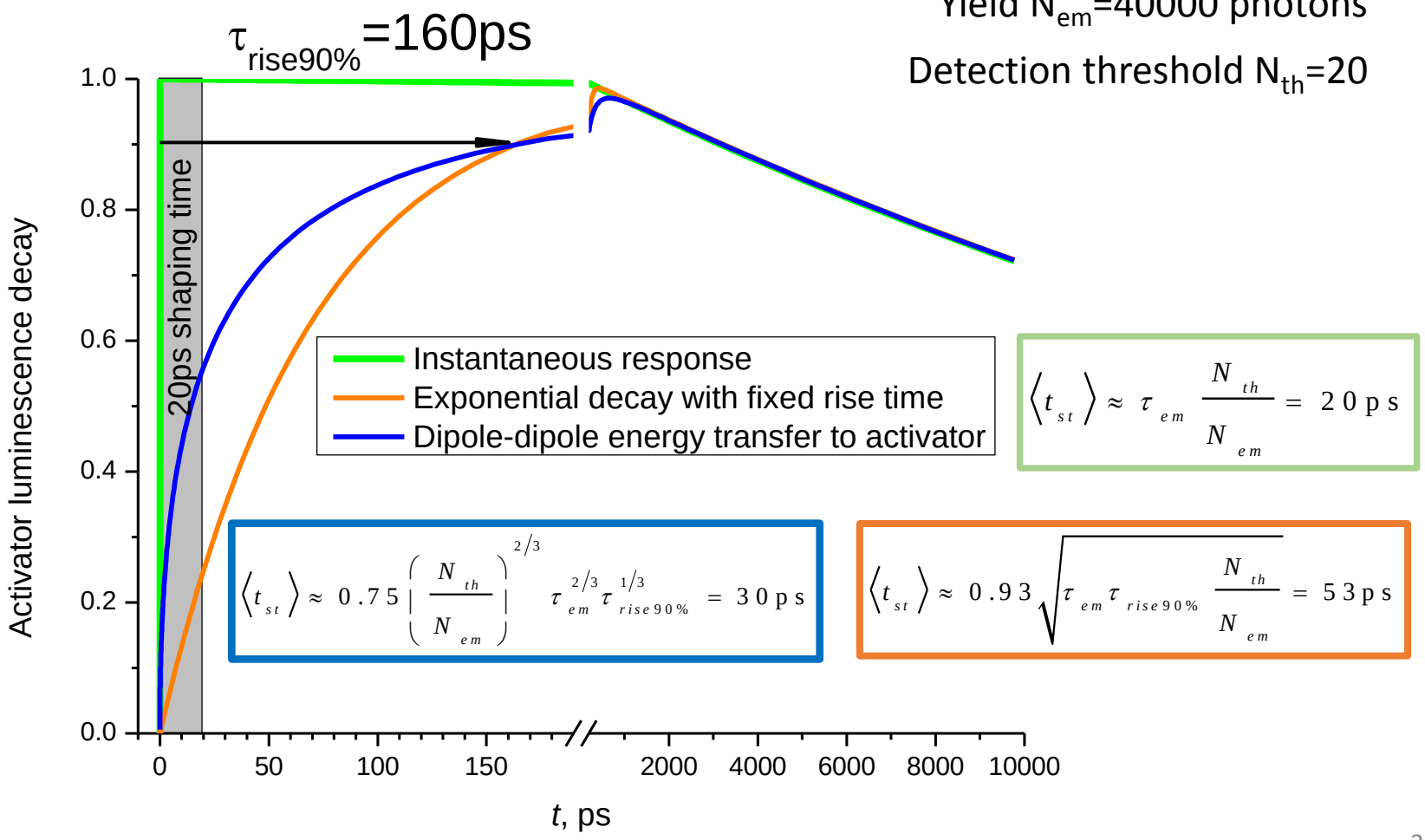

Structure of rise time for activator emission

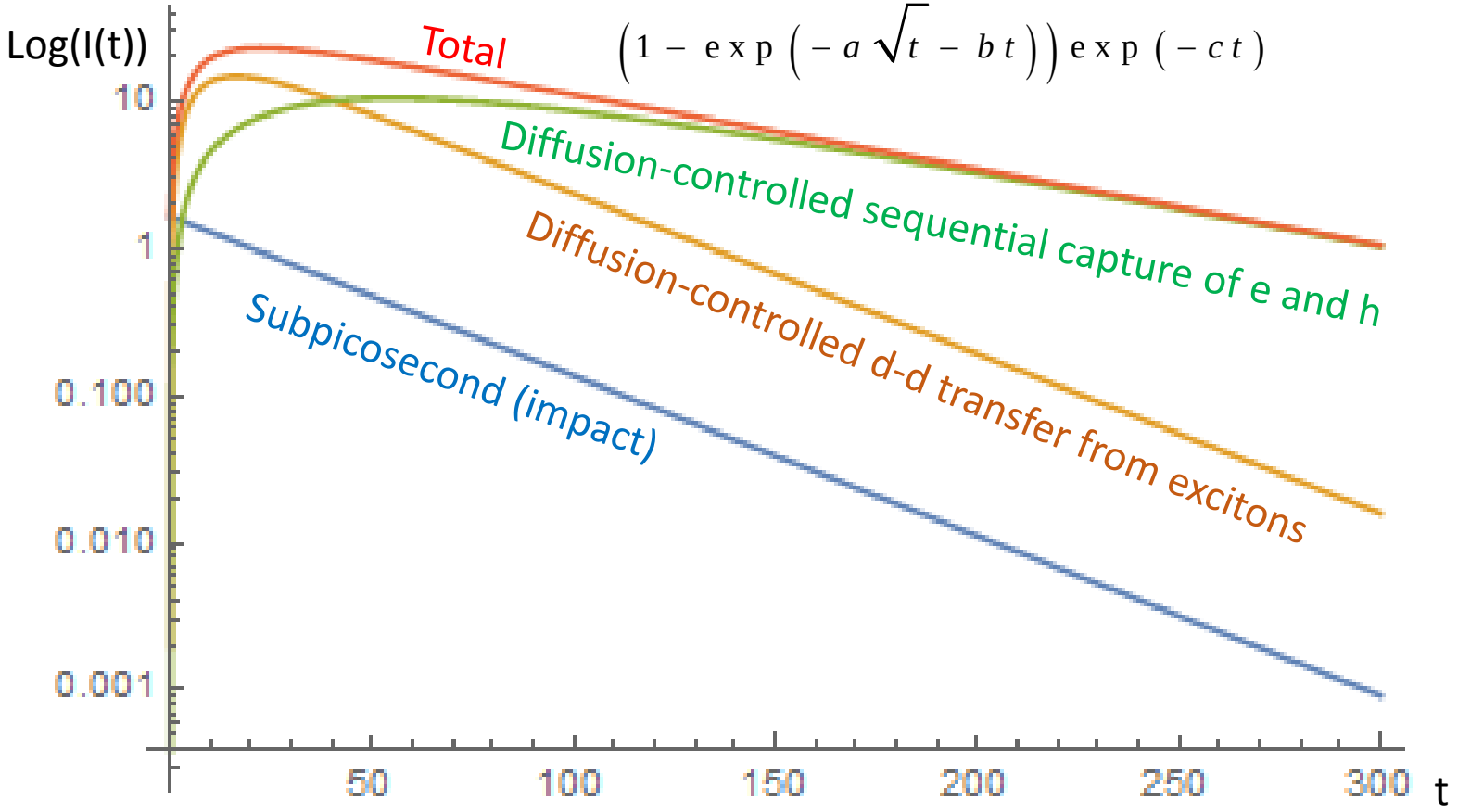

Fast energy transfer from hot (free) carries

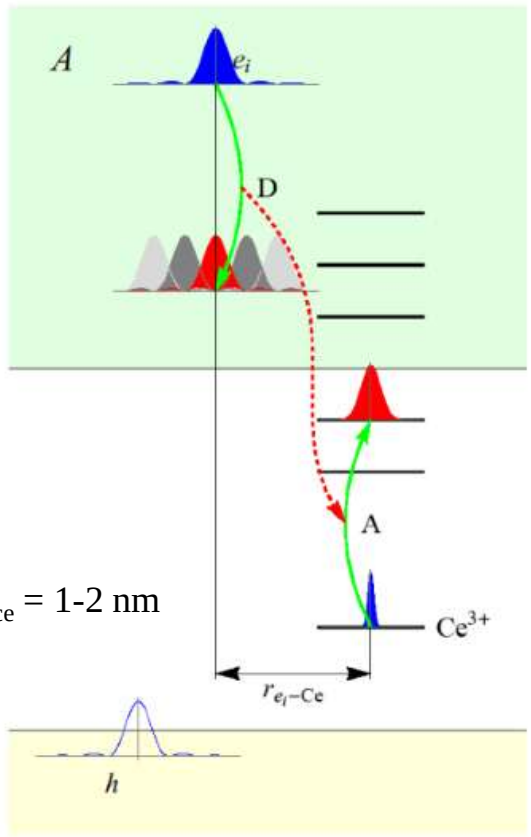

$r_{e\text{-}ce}$ = 1-2 nm

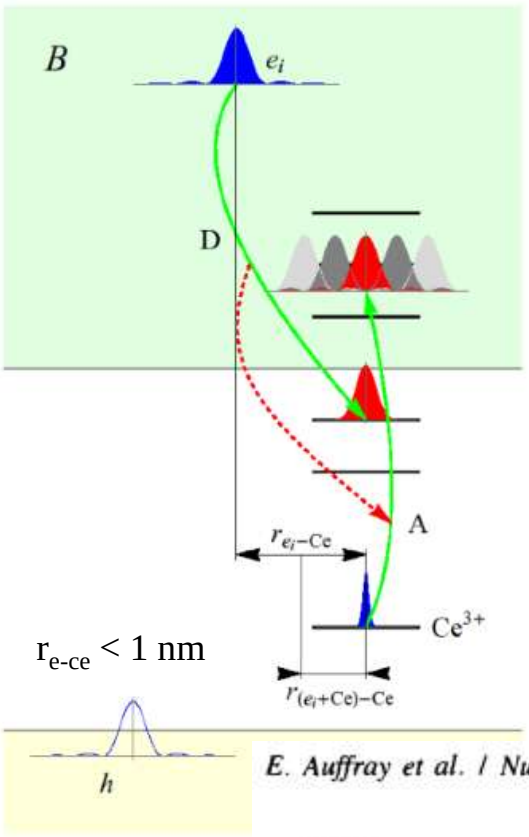

$r_{e\text{-}ce}$ < 1 nm

Filled waveforms represent electrons, open waveforms – holes. Initial states are shown in blue, final – in red.

Need very high Ce^{3+} concentration!

E. Auffray et al. / Nucl. Instr. and Meth. in Phys. Res. A 383 (1996) 367–393

Impact hot excitation of Ce^{3+} ions: Left – due to dipole-dipole process (Förster type), right – due to exchange process (Dexter type).

Linear in density of excitations

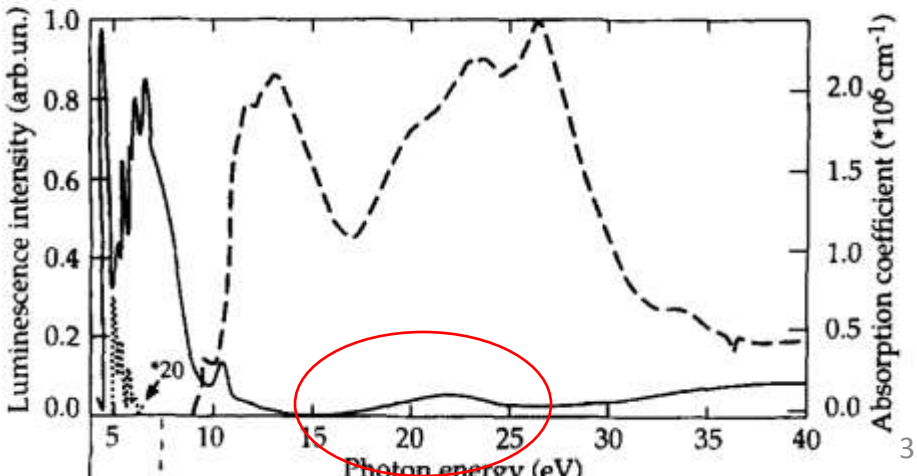

Fast capture of exciton (free exciton, STE, correlated e-h pair)

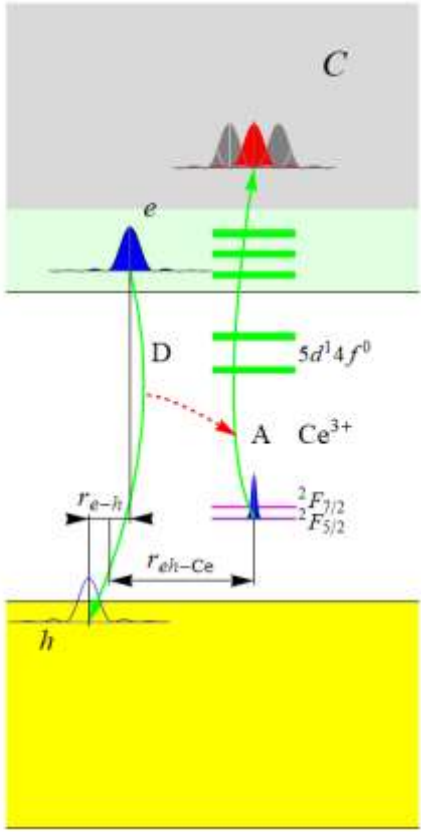

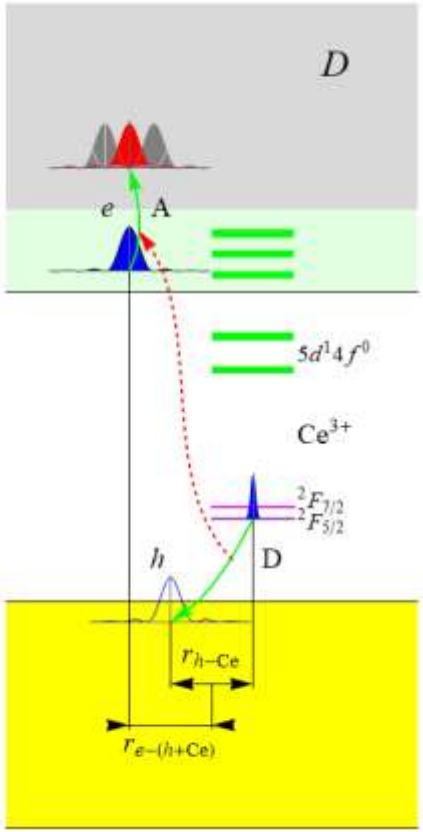

d-d transfer (Förster)

Exchange transfer (Dexter)

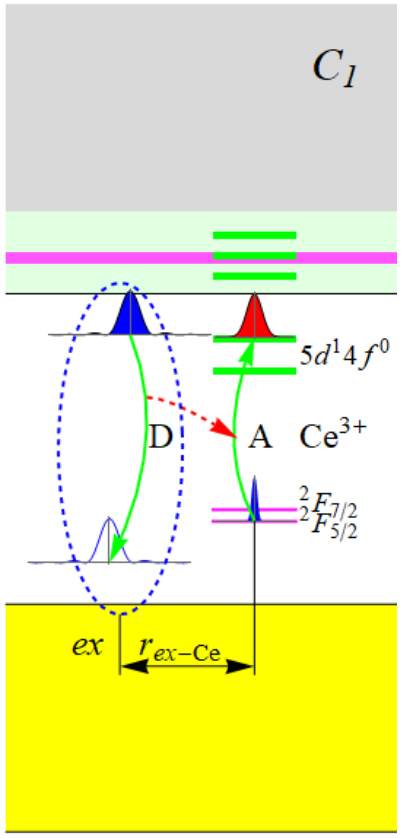

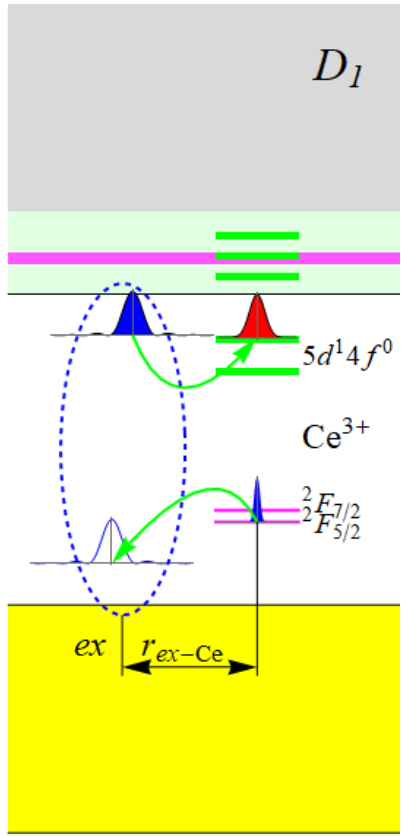

d-d transfer (Förster)

Exchange transfer (Dexter)

Free exciton and correlated e-h pair

STE

r_{e-h} <0.5nm, r_{eh-Ce} =2-3nm r_{h-Ce} <0.5nm, r_{e-Ce} =1-2nm

r_{e-h} <0.5nm, r_{eh-Ce} =2-3nm r_{h-Ce} <0.5nm, r_{e-Ce} =1-2nm

$FE+Ce^{3+} \rightarrow Ce^{4+}+e$

$STE+Ce^{3+} \rightarrow Ce^{4+}+e$, Ce^{3+*}

Fast capture of electron by Ce^{4+}

Nonlinear in density of excitations if additional Ce^{4+} are created due to $h+Ce^{3+}$ and $FE+Ce^{3+}$ processes

Important in case of presence Ce^{4+} in non-excited crystal due to divalent codoping

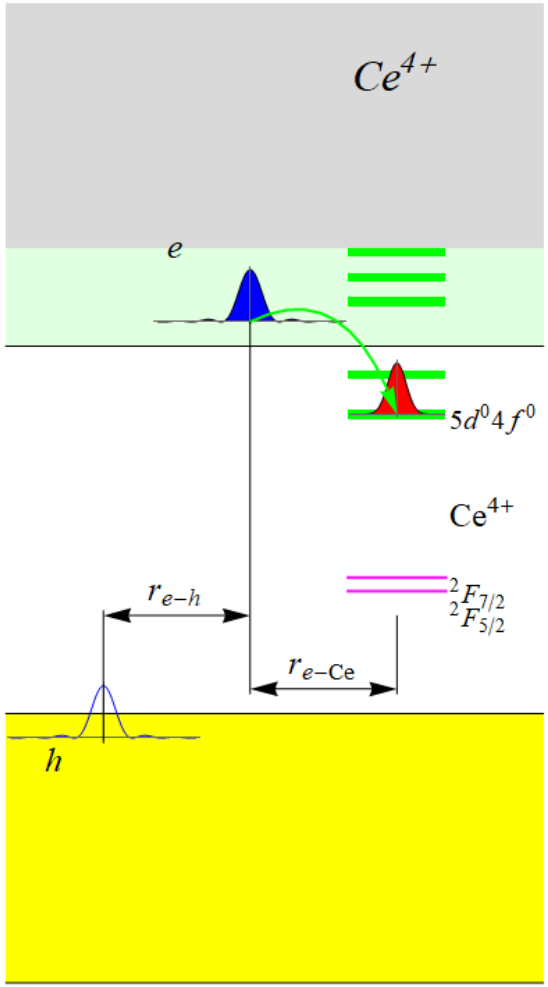

$\beta_{e+Ce4+} = 4\pi D_e R_{Onsager}$

$R_{onsager}$~10nm

$\beta_{e+Ce4+} >> \beta_{FE+Ce3+} >> \beta_{STE+Ce3+}$

$Ce^{4+} + e \rightarrow Ce^{3+*}$

See G.Tamulatis talk

Example of spatial distribution of electrons and holes in CsI after thermalization

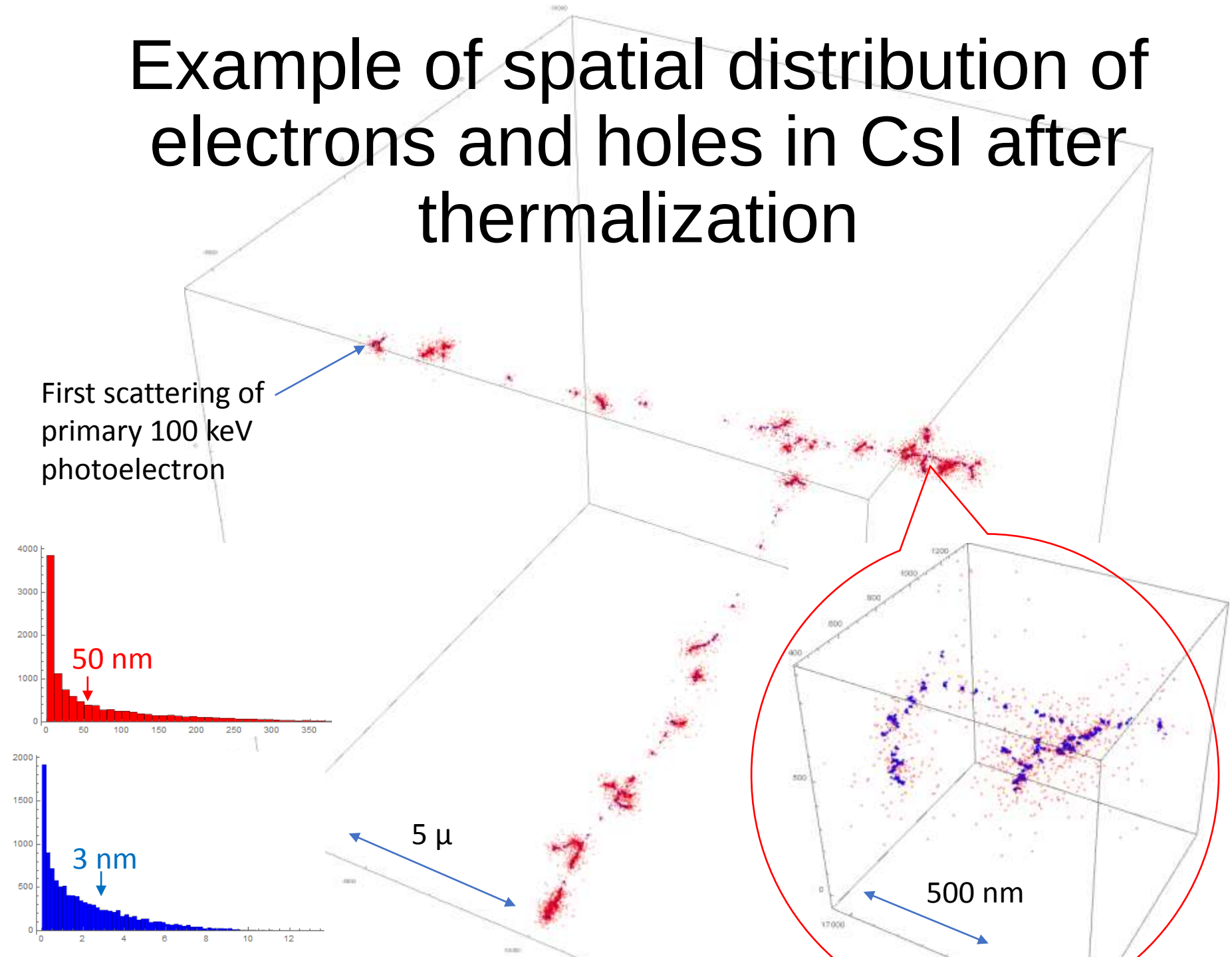

Kinetics of recombination significantly depends on initial concentration of excitations:

Low concentrations, rising part of kinetics, hyperbolic long tails, $n<10^{16}$ cm^{-3}

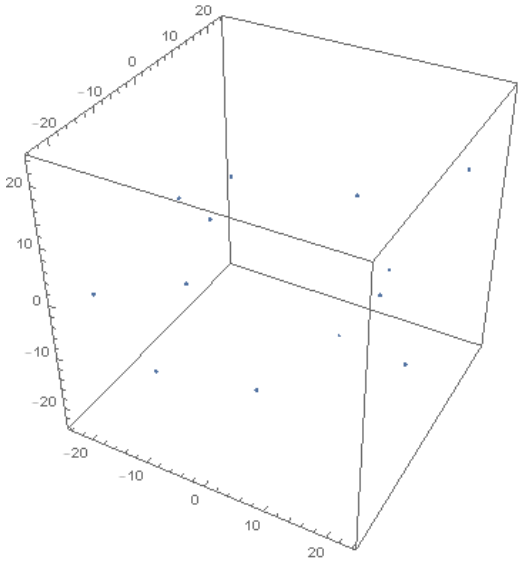

Medium concentrations without quenching, rather fast recombination

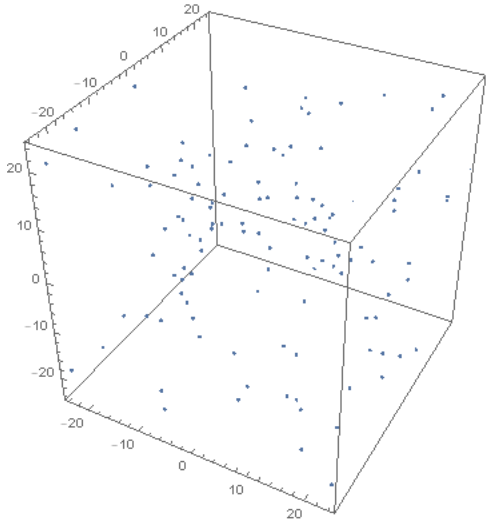

High concentrations, strong quenching of excitations, fast initial decay stage, $n>10^{19}$ cm^{-3}

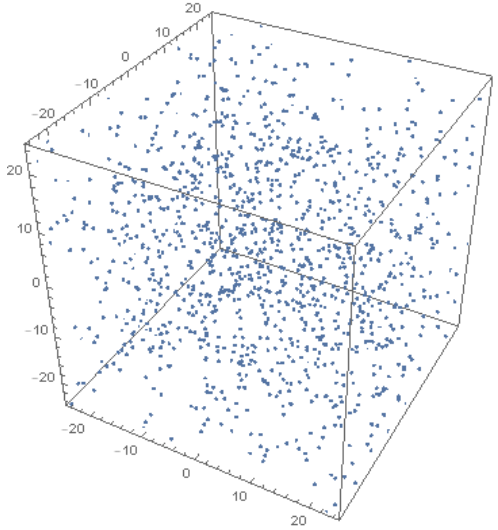

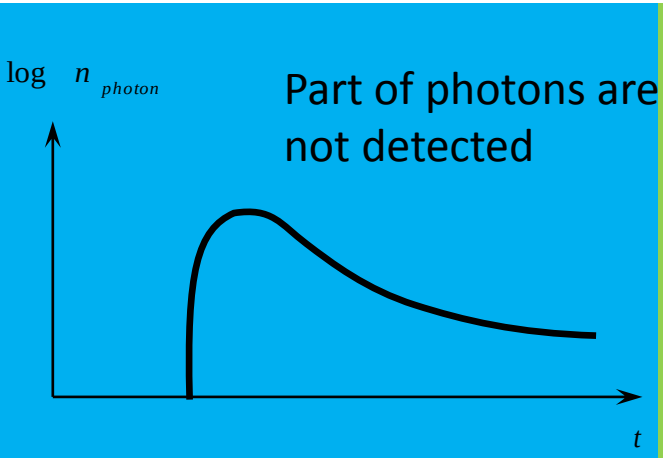

Part of photons are not detected

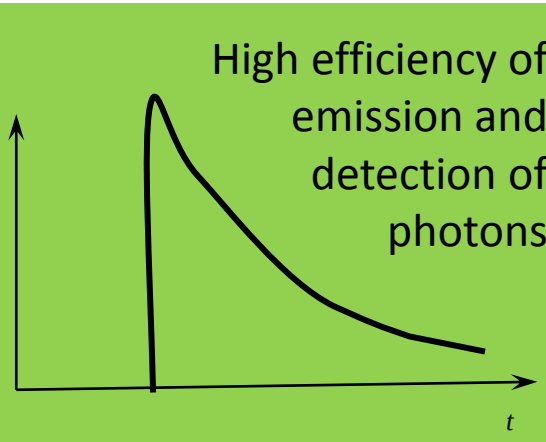

High efficiency of emission and detection of photons

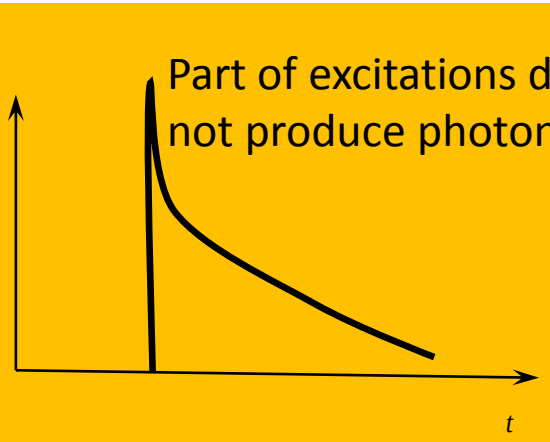

Part of excitations do not produce photons

How to define “concentration”?

For uniform random distribution:

$$\left\langle r_{ee} \right\rangle \approx n^{-1/3}$$

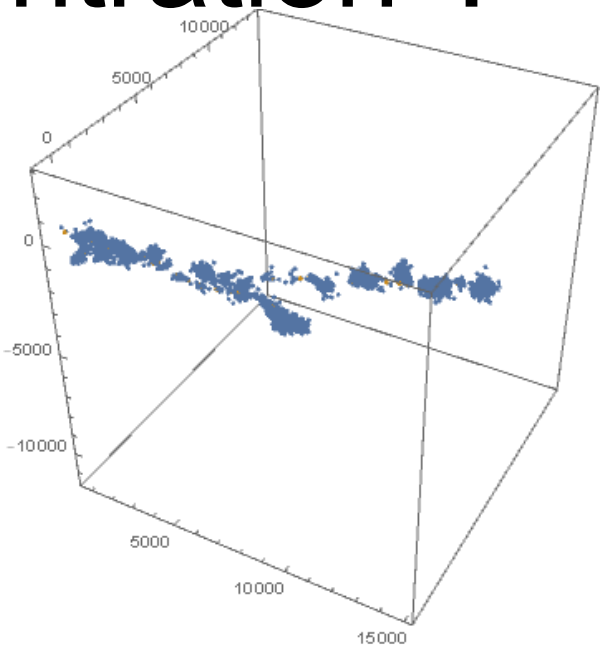

For track structure:
“Concentration” which “feel” a particle:

$$n \approx \left\langle r_{ee} \right\rangle^{-3}$$

for three closest particles

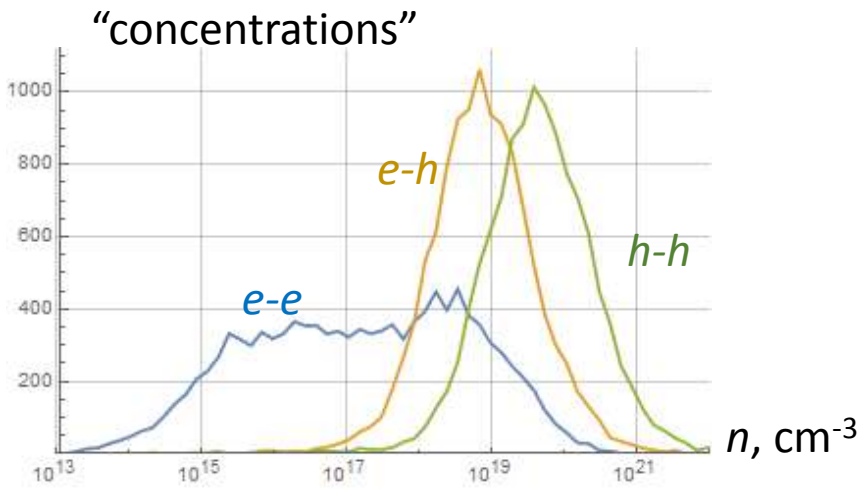

Distribution of e-h concentration in track region

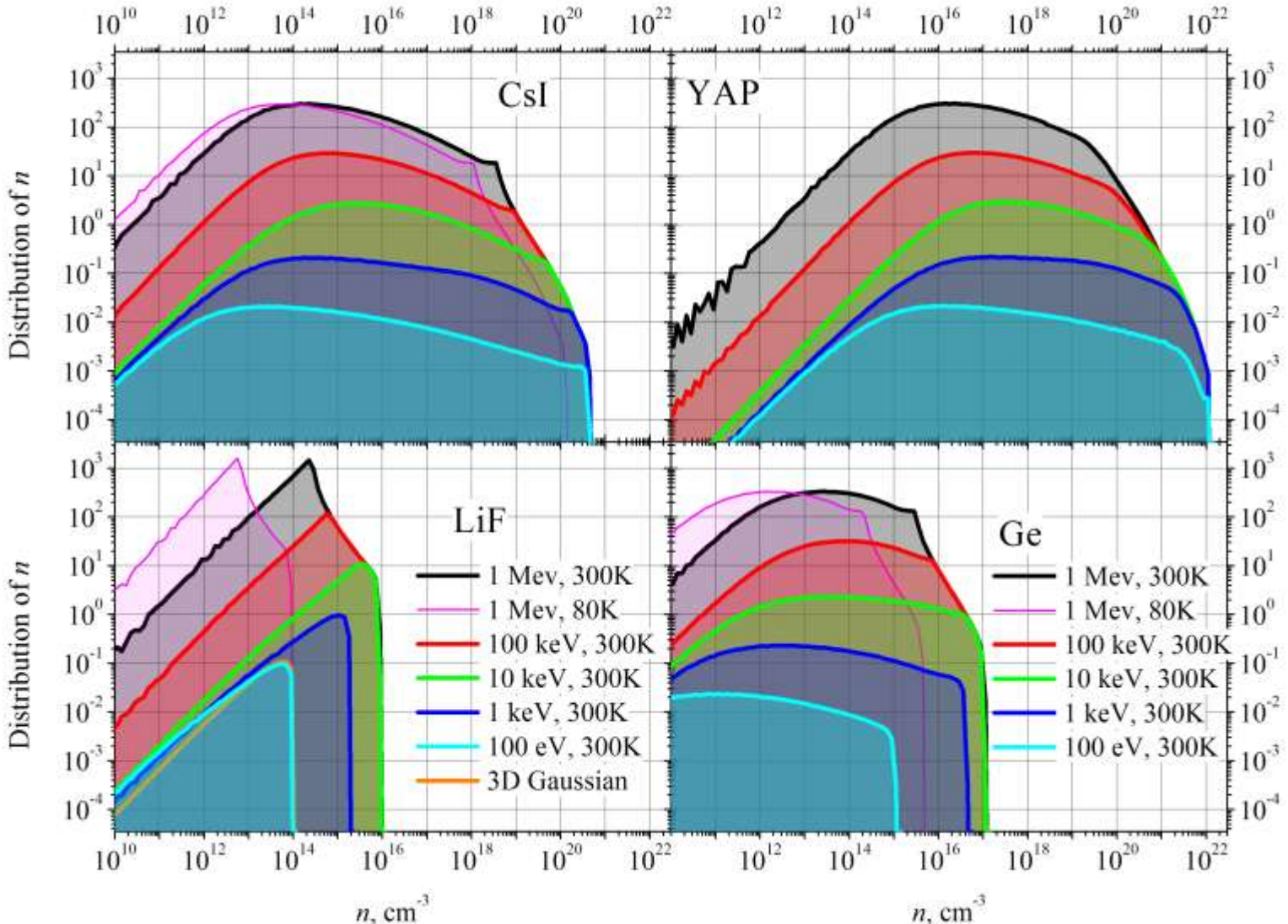

The balance of two e-transfer channels is controlled by the density of excitations (n_{Ce3+}=0.2%)

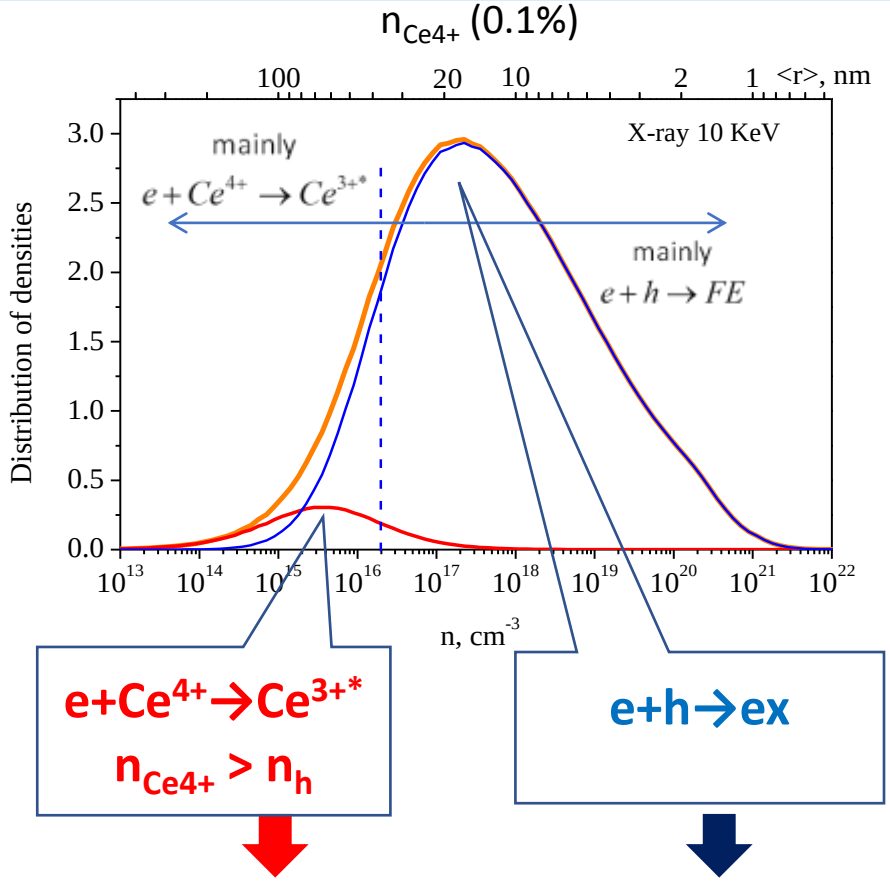

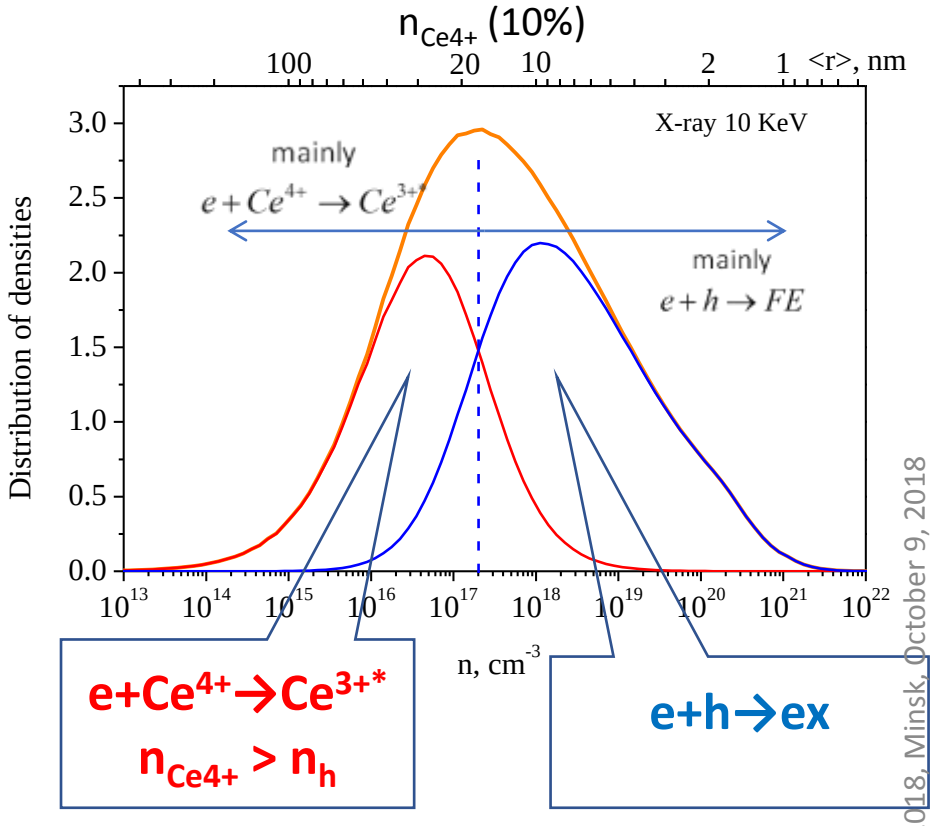

$$\frac{dn_e}{dt} = -4\pi D_e R^{scr}_{Ons} n_{Ce^{4+}} n_e - 4\pi (D_e + D_h) R^{scr}_{Ons} n_h n_e - \cdots$$

Ce^{4+} captures an electron in low density part of track

Excitons are created in high density part of track and transfer their energy to Ce^{3+}

A.Belsky et al, EURODIM2018, Bydgoszcz

A.Vasil'ev, ISMART2018, Minsk, October 9, 2018

Quenching of excitons in high density area

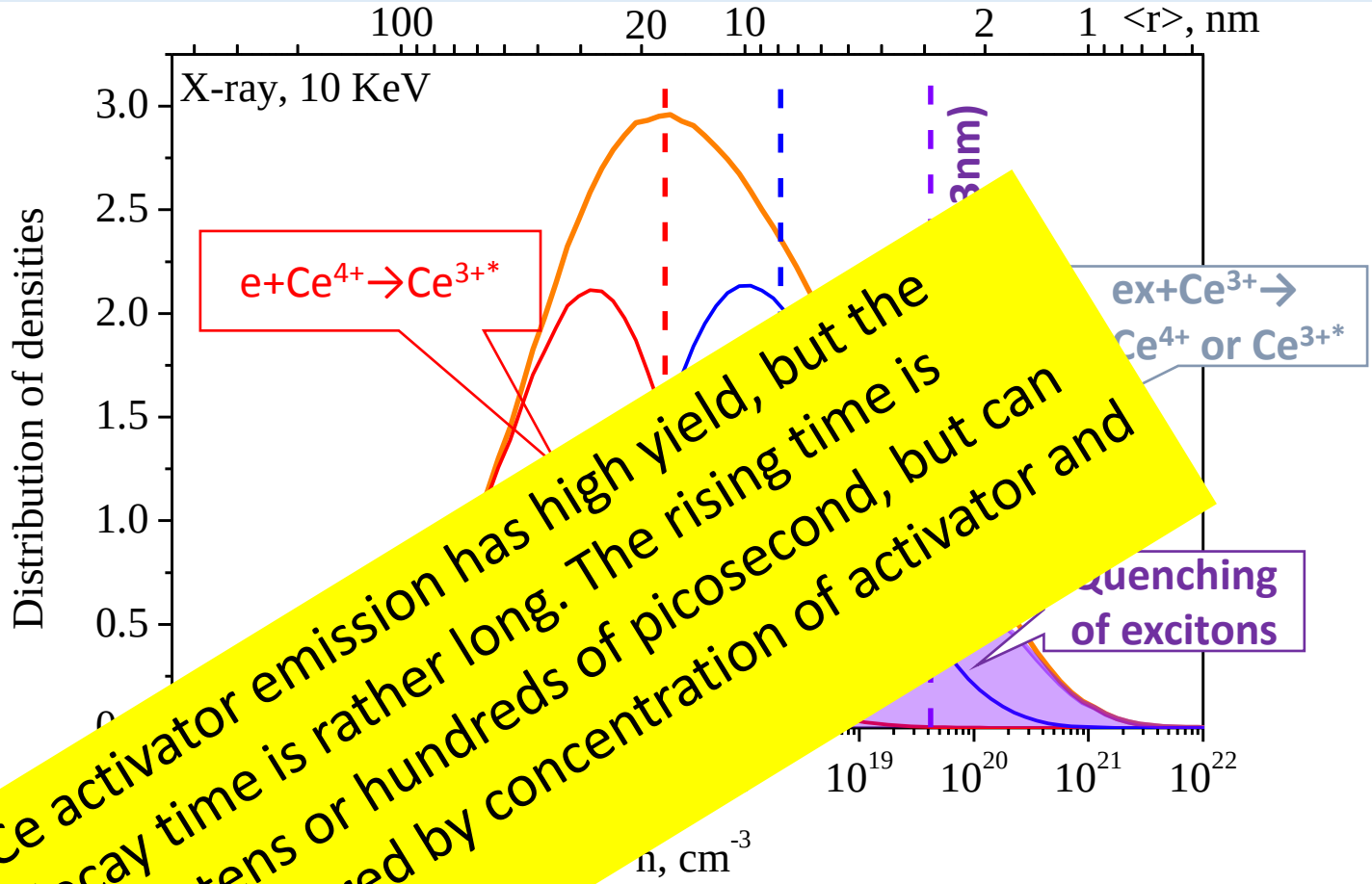

Ce activator emission has high yield, but the decay time is rather long. The rising time is about tens or hundreds of picosecond, but can be engineered by concentration of activator and co-activators.

Th efore the transfer to cerium is important sou in scintillation mechanism. As consequence the transf to Ce^{3+} decreases. The excited cerium created from Ce^{4+} by pture in low density region is less affected by these losses.

The increase of LY after conversion of Ce^{3+} in Ce^{4+} by Mg^{2+} co-doping can be explained by this effect.

A.Belsky et al, EURODIM2018, Bydgoszcz

Fast emission processes in regions of high concentration of excitations

Time-resolved luminescent z-scan of FIL: CsI. Decay vs density

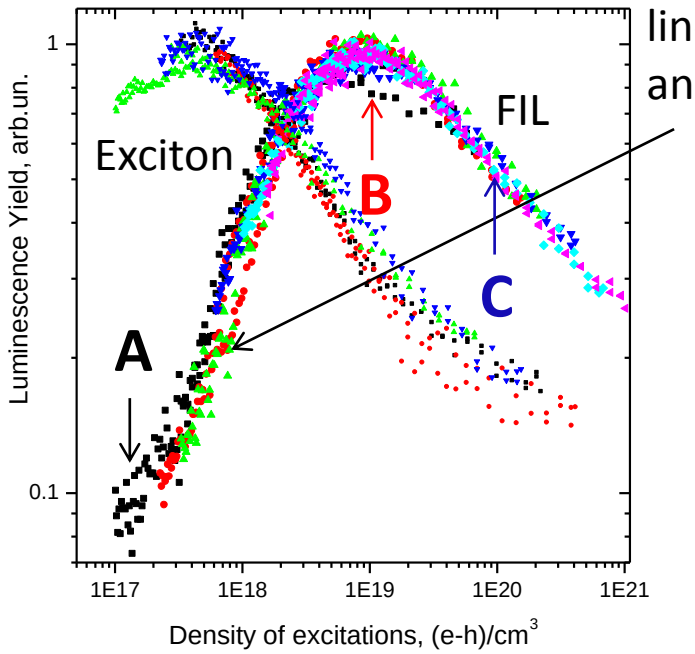

FIL LY increases linearly between 10^{17} and 10^{19} cm^{-3}.

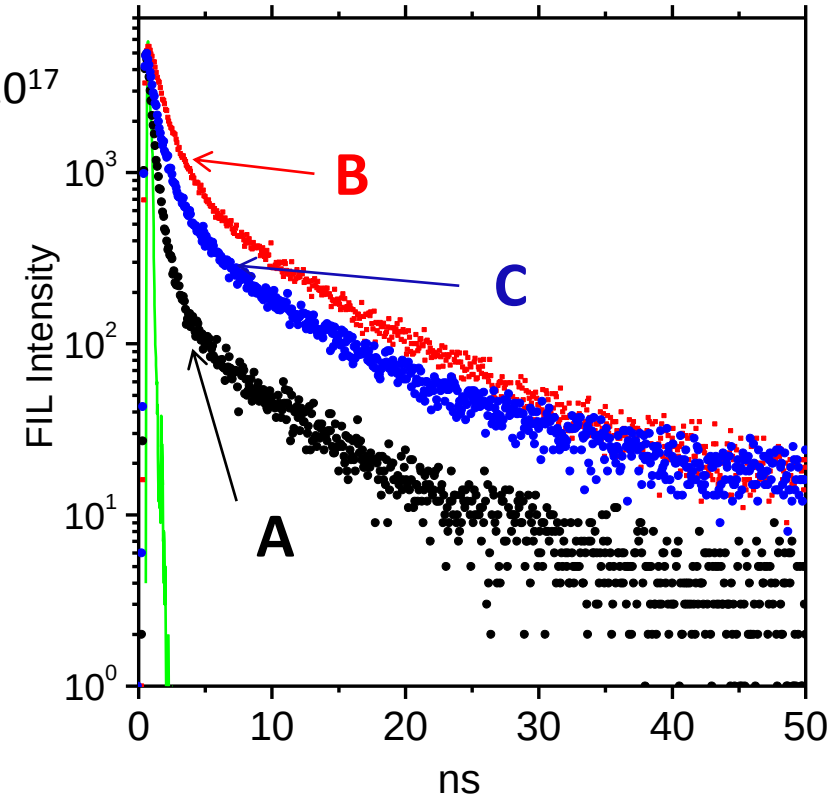

A – low density region – fastest decay – quenching profile

Model: low F, small SOC shift (ΔE is close to kT) - instability of FIL state

B - intermediate density region, decay becomes slower, max of LY and min of quenching

Model: relatively high F, ΔE> kT, more stable FIL centers

C – max density (focal point), quenching increases

Model: high F, ΔE>> kT, destruction of FIL center by interaction with other excitations

A.Belsky et al, LUMDETR2018, Prague

Time-resolved luminescent z-scan of free excitons: ZnO

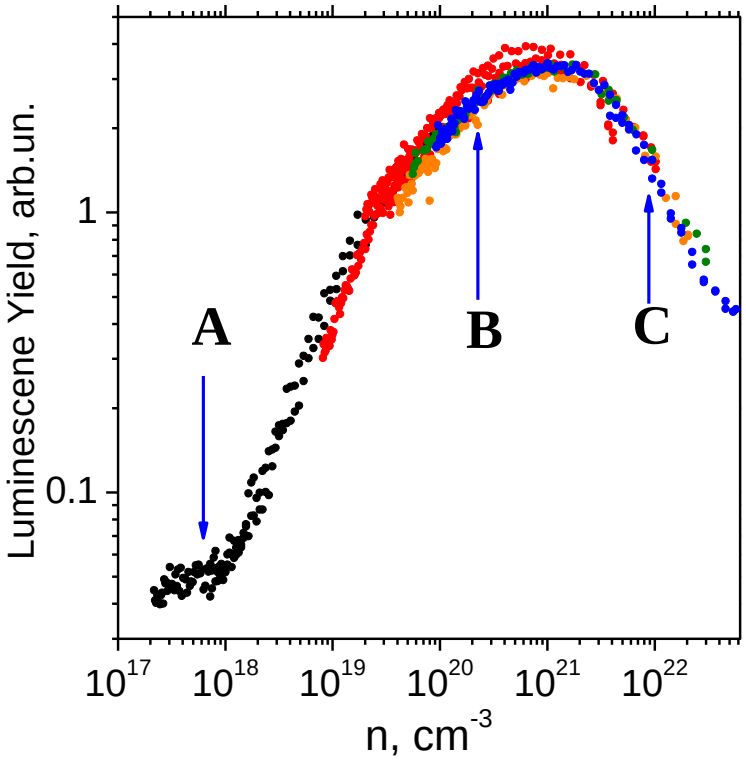

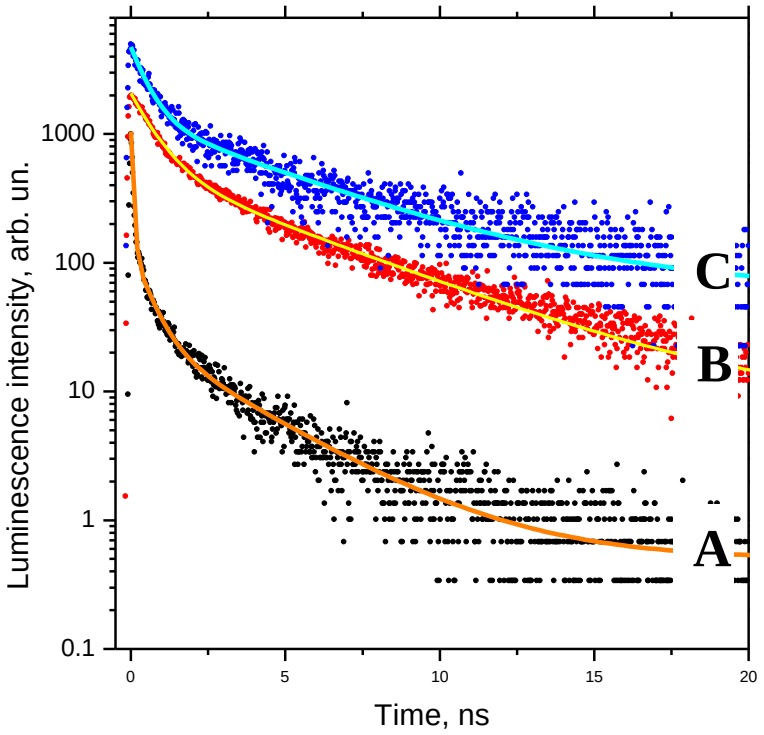

ZnO and CsI have quite different properties, but time-resolved z-scans are similar. In particular decay curves show the same trends.

A.Belsky et al, LUMDETR2018, Prague

Luminescent z-scan of FIL: $CsPbCl_3$

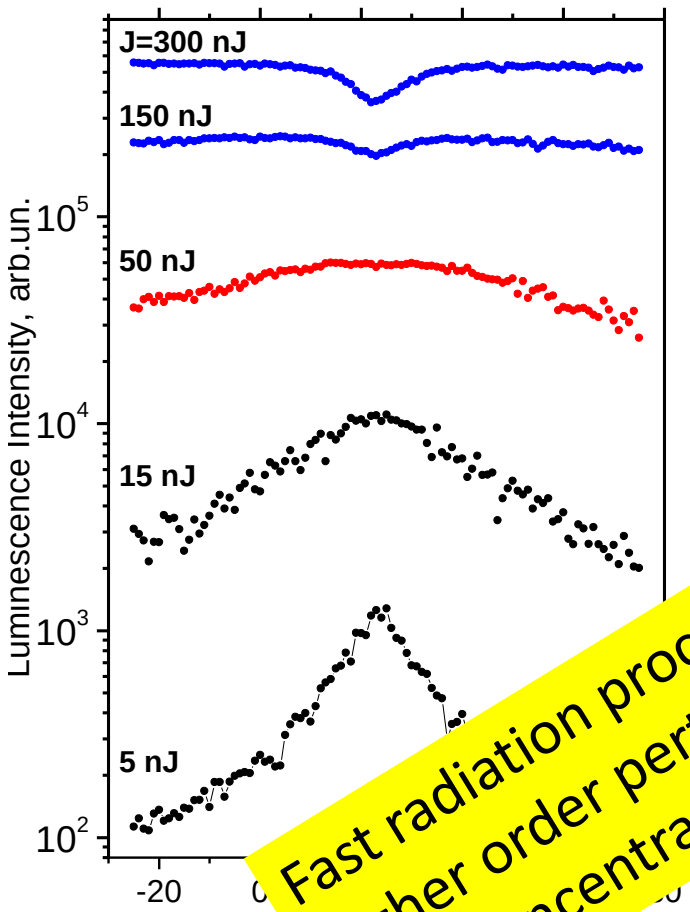

Z-scan curve specific to FIL response

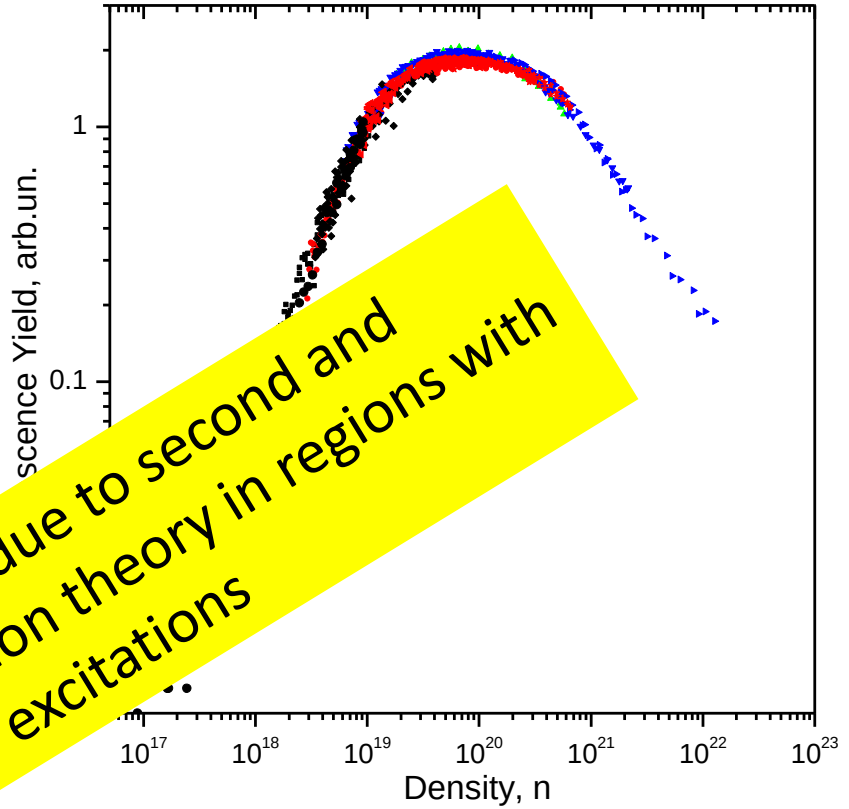

Fast radiation processes due to second and higher order perturbation theory in regions with high concentration of excitations

FIL LY vs excitation density

	Saturation	Quenching
CsI	4×10^{18} cm^{-3}	2×10^{19} cm^{-3}
ZnO	3×10^{20} cm^{-3}	2×10^{21} cm^{-3}
$CsPbCl_3$	10^{19} cm^{-3}	10^{21} cm^{-3}

A.Belsky et al, LUMDETR2018, Prague

Fast emission processes with nanostructured heavy crystals

Two additional values by using nanoparticles

- Faster emission from nanoparticles
- Nanoparticles in nanocomposites as radiation transformers

Confinement and excitons

- Bi-exciton emission in nanocrystrals:
  - Bi-excitons have faster radiation time in comparison with conventional excitons
  - Bi-excitons can be produced directly by ionizing particle
  - Bi-excitons in nanoparticles can exist for longer time due to confinement
  - Bi-excitons emission is destroyed by Auger processes

Confinement and excitons

- Bi-exciton emission in nanocrystrals:
  - Bi-excitons have faster radiation time in comparison with conventional excitons
  - Bi-excitons can be produced directly by ionizing particle
  - Bi-excitons in nanoparticles can exist for longer time due to confinement
  - Bi-excitons emission is destroyed by Auger processes

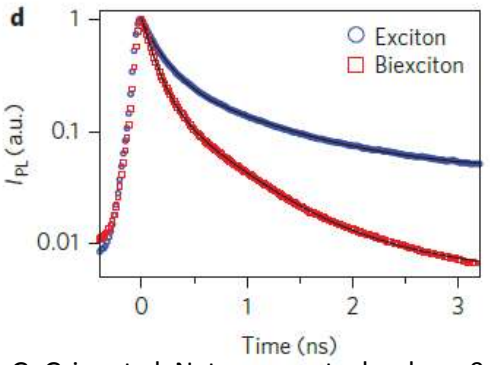

G. Grim et al, Nature nanotechnology, 9 (2014) 891-895

$$\tau_{XX} \approx \tau_X / 4$$

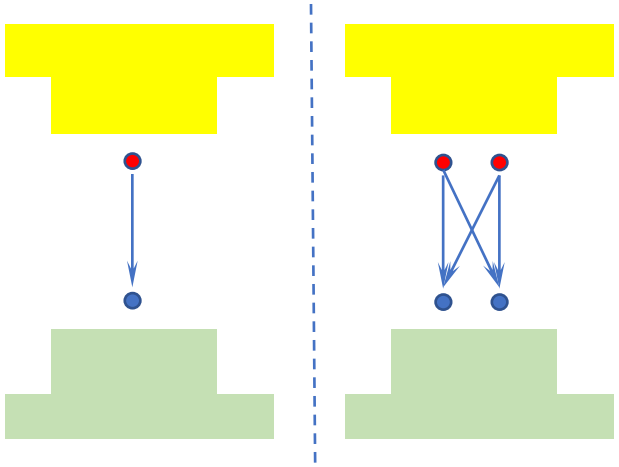

Confinement and excitons

- Bi-exciton emission in nanocrystrals:
  - Bi-excitons have faster radiation time in comparison with conventional excitons
  - Bi-excitons can be produced directly by ionizing particle
  - Bi-excitons in nanoparticles can exist for longer time due to confinement
  - Bi-excitons emission is destroyed by Auger processes

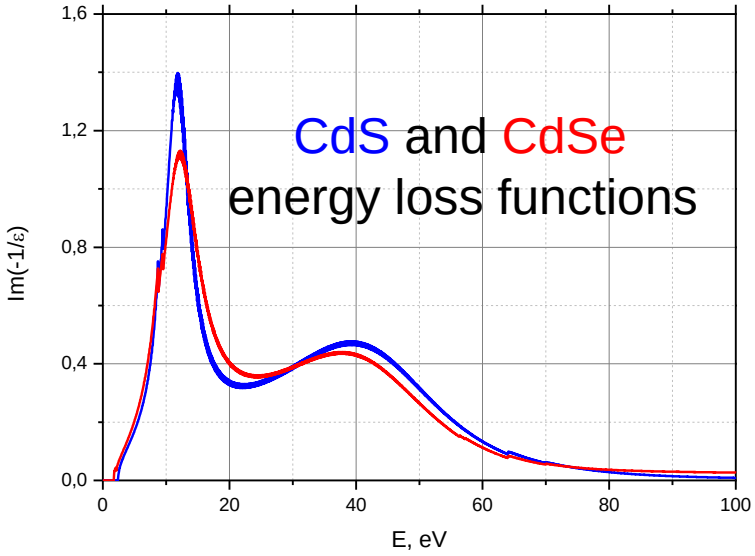

$$\hbar\omega_{pl} >> E_g$$

$$\hbar\omega_{pl} \rightarrow 2e + 2h \text{ or even } 3e + 3h$$

Confinement and excitons

- Bi-exciton emission in nanocrystrals:
  - Bi-excitons have faster radiation time in comparison with conventional excitons
  - Bi-excitons can be produced directly by ionizing particle
  - Bi-excitons in nanoparticles can exist for longer time due to confinement
  - Bi-excitons emission is destroyed by Auger processes

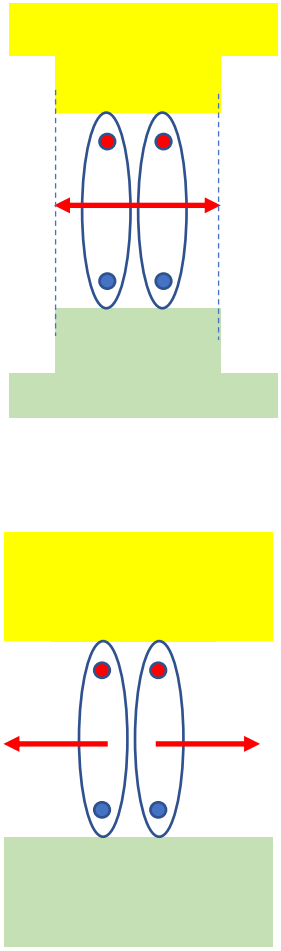

Confinement and excitons

- Bi-exciton emission in nanocrystrals:
  - Bi-excitons have faster radiation time in comparison with conventional excitons
  - Bi-excitons can be produced directly by ionizing particle
  - Bi-excitons in nanoparticles can exist for longer time due to confinement
  - Bi-excitons emission is destroyed by Auger processes

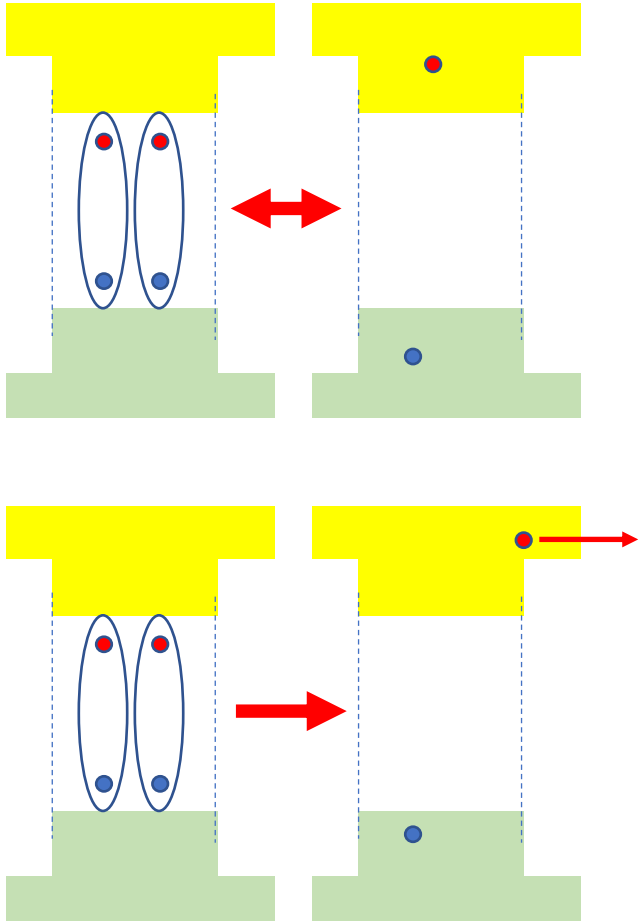

Nanocomposites

- Nanoparticles as transformers of ionizing radiation into electrons, which in turn can excite polymer matrix

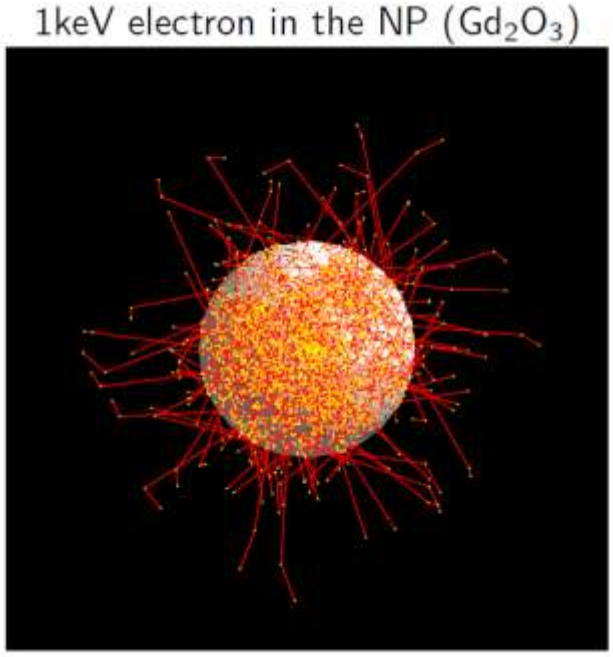

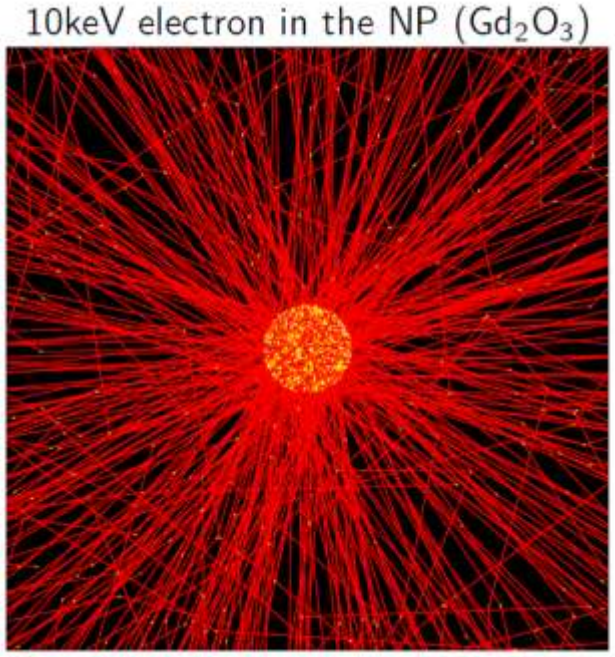

A.-L. Bulin et al, Nanoscale 2015

C.Dujardin et al, LUMDETR2018, Prague

Estimation of electron escape from CdSe nanoparticles

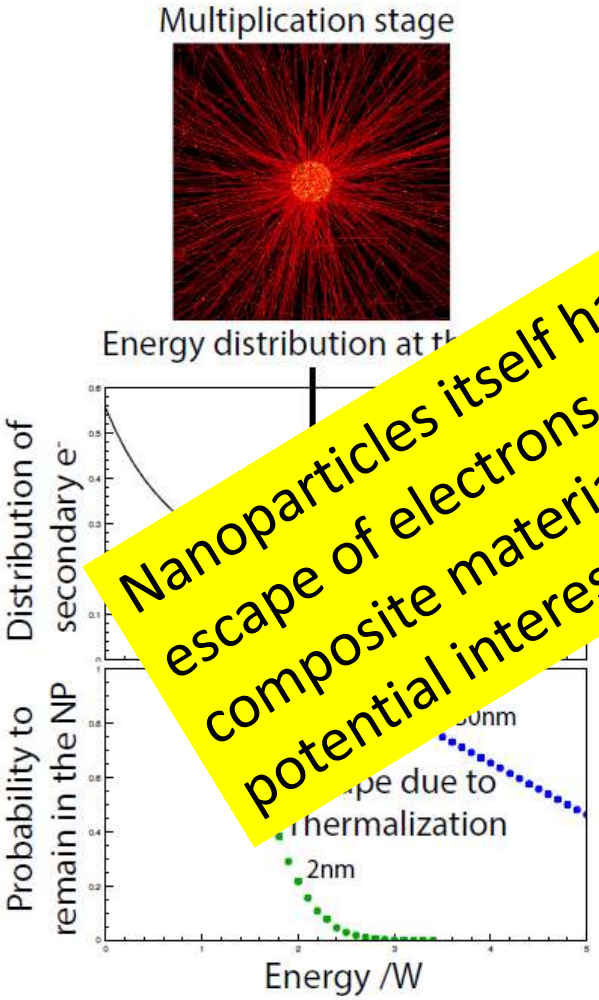

Nanoparticles itself have low yield due to escape of electrons and charging. Nevertheless, composite materials with polymer matrix are of potential interest for fast timing.

of the
tside of the
al nanoscale 2015)
Se nanocrystal as:
rk function, $W = 10\hbar\Omega_{LO}$
$E_g = 5W$

- microtheory allows to estimate the energy distribution of the electron
- and to evaluate the escape
- 30 nm $\rightarrow$ 47% of escape
- 2 nm $\rightarrow$ 90% of escape

C.Dujardin et al, LUMDETR2018, Prague

Conclusions

- Quenched luminescence is highly welcome for fast timing, but provide poor energy resolution
- IBL with gaps of about 1 eV (CL) is still promising
- High cerium concentration could make rise time shorter (concentration quenching should not increase the rise time)
- Nanoparticles embedded into polymer matrices can be interesting candidates for fast timing
- Crystals with nonlinear emission (ZnO, $CsPbCl_3$ and pure CsI) are also promising

Thank you for your attention!

Many thanks to Intelum, FAST and
CCC communities and support!

This research is carried out in the frame of Crystal Clear Collaboration and is supported by a European Union's Horizon 2020 research and innovation program under the Marie Skłodowska-Curie grant agreement No 644260 (INTELUM) and COST ACTION TD1401 (FAST).